

Massive Spin-3/2 Rarita-Schwinger Quasiparticle in Condensed Matter Systems

Feng Tang^{1,4,*}, Xi Luo^{2,*}, Yongping Du^{5,1,4}, Yue Yu^{3,4}, and Xiangang Wan^{1,4}

¹*National Laboratory of Solid State Microstructures and School of Physics, Nanjing University, Nanjing 210093, China*

²*CAS Key Laboratory of Theoretical Physics, Institute of Theoretical Physics, Chinese Academy of Sciences, Beijing 100190, China*

³*State Key Laboratory of Surface Physics, Center for Field Theory and Particle Physics, Department of Physics, Fudan University, Shanghai 200433, China*

⁴*Collaborative Innovation Center of Advanced Microstructures, Nanjing 210093, China and*

⁵*Department of Applied Physics, Nanjing University of Science and Technology, Nanjing 210094, China*

(Dated: September 5, 2017)

The spin-3/2 elementary particle, known as Rarita-Schwinger (RS) fermion, is described by a vector-spinor field $\psi_{\mu\alpha}$, whose number of components is larger than its independent degrees of freedom (DOF). Thus the RS equations contain nontrivial constraints to eliminate the redundant DOF. Consequently the standard procedure adopted in realizing relativistic spin-1/2 quasi-particle is not capable of creating the RS fermion in condensed matter systems. In this work, we propose a generic method to construct a Hamiltonian which implicitly contains the RS constraints, thus includes the eigenstates and energy dispersions being exactly the same as those of RS equations. By implementing our 16×16 or 6×6 Hamiltonian, one can realize the 3 dimensional or 2 dimensional (2D) massive RS quasiparticles, respectively. In the non-relativistic limit, the 2D 6×6 Hamiltonian can be reduced to two 3×3 Hamiltonians which describe the positive and negative energy parts respectively. Due to the nontrivial constraints, this simplified 2D massive RS quasiparticle has an exotic property: it has vanishing orbital magnetic moment while its orbital magnetization is finite. Finally, we discuss the material realization of RS quasiparticle. Our study provides an opportunity to realize higher spin elementary fermions with constraints in condensed matter systems.

I. INTRODUCTION.

By requiring the Lorentz invariance and a positive probability density, Dirac proposed in 1928 a relativistic wave equation [1]. Describing spin-1/2 particles, this equation is known as the Dirac equation [1]. In 1929, Weyl introduced Weyl equation, a simplified version of the Dirac equation for relativistic particles, whose solutions predicted massless fermions with a definite handedness (or chirality) [2]. The third relativistic quantum mechanical equation for spin-1/2 fermion is Majorana equation, and the antiparticle of Majorana fermion is itself [3]. It is well known that Dirac equation describes electrons etc. However, Weyl and Majorana fermions have not been observed as an elementary particle in the laboratory or nature yet. In spite of the huge energy-scale difference, currently the rich correspondences between high energy physics and condensed matter (CM) physics attract a lot of research attentions. Several unique electronic structures in certain CM systems (CMS) behave analogously to elementary particles. For instance, the Dirac quasi-fermions in graphene [1, 4–6] and Dirac semimetals [7–9]. The Weyl quasiparticle was proposed [10–15] and has been experimentally confirmed in Weyl semimetals [16–18]. The Majorana zero modes in CMS were also discussed intensively [19–21].

It is worth emphasizing that the properties of these quasiparticles in CMS are much more flexible and fruitful than their high energy counterparts: (i) The finite

size of the system gives these quasiparticles the chance to see the peculiar edge and surface states of the world [10, 22, 23]. (ii) The minimal spacing of the lattice makes them safe from the ultraviolet divergence. (iii) Novel tunneling properties associated with Klein paradox may be experimentally examined [6]. (iv) The effect of the chiral anomaly can be evaluated by highly anisotropic negative magnetoresistance [24, 25]. (v) There are quasiparticles with non-abelian statistics [19], which may be applied to topological quantum computation [26].

Without exhaustively listing the intriguing features of the spin-1/2 relativistic quasiparticles in CMS, however, the basic properties of these spin-1/2 fermions have been adequately studied and well-understood. On the other hand, the relativistic particles with spin higher than one appear neither as elementary particles nor as quasiparticles in CMS, although they were studied in the early day of quantum mechanics [27]. Especially, the spin-3/2 fermion, which obeys Rarita-Schwinger (RS) equations [28], plays a key role in supergravity theory [29]. Very recently, by considering the fourfold degenerate band crossing points, the possible spin-3/2 generalization of the Dirac equation in CMS were proposed [30–33]. Instead of the shackle from Lorentz invariance in quantum field theory, these quasiparticles are only subject to the crystallographic symmetry groups. Therefore, one can classify the band crossing points which are stabilized by space group symmetries and then search for the possible quasi-fermions that have no counterparts in high energy physics [30, 34–39].

Among the interesting properties of the RS fermion, the most astonishing one is that external magnetic field can induce a superluminal mode for the massive RS (M-

*These two authors contribute equally.

RS) fermion [40, 41]. The “speed of light” which is usually the Fermi velocity in CMS is not the upper limit of the quasiparticle velocity and thus the “superluminal” modes and “acausality” are basically permitted. The two dimensional (2D) M-RS gas also shows a nonlinear quantum Hall phenomenon [42] which is different from the well-known quantum Hall effects in the 2D electron gas [43] and the Dirac fermion gas in graphene [44]. Therefore, to create the M-RS quasiparticles in CM playground is a very intriguing topic, which we address in this work. Inspired by the CM simulation of the Dirac fermion[45], we aim to construct a Hamiltonian with the wave function and the corresponding energy dispersion around the Fermi level approximately the same as the relativistic spin-3/2 RS particles. Thus the low-lying excitations are the RS quasiparticles.

In high energy physics, it is convenient to use either equation of motion or Lagrangian, while Hamiltonian formalism is favored in CMS. To obtain the corresponding Hamiltonian for relativistic spin-1/2 particles is straightforward because their wave equations are the ones with first order time derivative. By requiring that the effective electronic Hamiltonian around some points in momentum space of CMS approximately the same as the Hamiltonian in high energy physics, one can realize spin-1/2 relativistic fermions (such as Dirac, Weyl and Majorana fermion) in CMS as emergent phenomena. However, the wave function of spin-3/2 M-RS fermions, represented by a vector-spinor ψ_μ , are of 16 or 6 components for d ($d = 3$ or 2) dimensional systems, while the number of the genuine degrees of freedom (DOF) are only 8 or 2 [46]. Thus, in addition to first order time derivative equations, RS equations also contain constraint equations, which do not exist for spin-1/2 fermions, to eliminate the redundant DOF.

The Hamiltonian for high-spin relativistic fermions has also been derived [47]. However in addition to the Hamiltonian [47], which is only for the genuine DOF, one still needs to explicitly include the constraint equations to obtain all the components of RS wave function ψ_μ to completely solve the RS particle problem as shown in the following section. Thus one cannot simply use this Hamiltonian[47] and follows the standard procedure adopted in spin-1/2 fermions to realize the spin-3/2 quasiparticle in CMS. In order to realize relativistic RS excitations in CMS, in this work for 3D (or 2D) we construct a 16-band (or 6-band) Hamiltonian which implicitly includes the RS constraint conditions. Such a Hamiltonian contains the eigen-solutions which are exactly the same as those of RS fermion. Since the dimension of our Hamiltonian is larger than the genuine DOF of the RS fermion, thus in addition to the RS modes, the proposed Hamiltonian also contains non-RS modes. We prove that these RS modes can be separated from the non-RS modes. By implementing our proposed 16×16 or 6×6 Hamiltonians in CMS, the 3D or 2D massive relativistic spin-3/2 RS quasiparticles can be realized. Focusing on the 2D case, which is much easier to realize

in realistic materials, we find that in the non-relativistic simplification with wavefunction approximated up to the first order of p/m , the 6×6 Hamiltonian can be reduced to two 3×3 matrices. We also find a novel property of these non-relativistic RS modes compared with those described by the Schrödinger and Dirac equations. In general, the Berry curvature and orbital magnetic moment formally have the same properties under the symmetry group. However for the 2D non-relativistic M-RS quasiparticles, we find that due to the nontrivial constraints on the RS quasiparticle, the Berry curvature is finite while the orbital magnetic moment vanishes. We also derive a sufficient condition which will restrict the orbital moment to be exactly zero. At last we search for the 2D non-relativistic M-RS quasiparticles around particular points in the Brillouin zone (BZ) and suggest the layered structures constructed from several trigonal and hexagonal lattices can hold such a low energy excitation. As an example, based on *ab initio* calculations, we predict that CaLiX (X=Ge and Si) are the candidates.

The paper is organized as follows. In Sec. II, we will present the Hamiltonian formalism of the massive high energy RS fermion in 2D and 3D. Realizing the non-trivial constraints of the RS fermions is the most difficult obstacle in CMS, and we propose a generic method to implicitly include these constraints in the effective Hamiltonian in Sec. III. We also give the 16×16 and 6×6 Hamiltonians which contain modes with the wavefunctions and energy spectra being exactly the same as the RS equations in Sec. III, so that one can realize 3D and 2D M-RS quasiparticles by implementing these Hamiltonian in CMS. Focusing on 2D case, we prove that in the non-relativistic approximation with wavefunction up to the first order of p/m , the positive and negative energy parts of RS wavefunctions decouples completely. Consequently the effective Hamiltonian for 2D RS quasiparticles can be reduced two 3×3 Hamiltonians in Sec. IV. In Sec. V, we show that due to the nontrivial constraints, this simplified 2D massive RS quasiparticle has an exotic property: although the intrinsic orbital magnetic moment of an energy band transforms like its Berry curvature under symmetry operations, the former is exactly zero-valued while the latter is finite. We also propose a possible material for the non-relativistic RS insulator in Sec. VI. Finally we summarize our results, comments on the par-tion construction and the topological classification of the non-relativistic RS insulator in the section of Discussions and Conclusions.

II. HAMILTONIANS OF RS FERMION FOR $d = 3$ AND 2 IN HIGH ENERGY PHYSICS.

The Lagrangian describing the massive relativistic spin- $\frac{3}{2}$ particles was first proposed by Rarita and Schwinger [28]. The corresponding equation of motion

reads

$$(\gamma \cdot \partial + m)\psi_{\mu\alpha} = 0, \quad (1)$$

$$\gamma \cdot \psi = \gamma_\mu \psi_\mu = 0, \quad (2)$$

which is a special case of Bargmann-Wigner (B-W) equation [48] that works for any arbitrary spin. The vector-spinor $\psi_{\mu\alpha}$ is of 16 or 6-components for $d = 3$ or 2 , μ is the vector index while α is the spinor index, and we choose the Dirac representation for the γ matrices and will omit the spinor index for later convenience. For the detailed description of the notations, see Secs. I and II of the SM [46]. With Eqs. (1) and (2), one can obtain a subsidiary condition $\partial \cdot \psi = 0$. This constraint and Eq. (2) project out the redundant spin-1/2 DOF and leave the genuine spin-3/2 ones.

In CMS, the momentum-space language is preferred. Thus we rewrite the RS equations (1) and (2) in the momentum space

$$i\partial_t \psi_\mu(\mathbf{p}, t) = (\boldsymbol{\alpha} \cdot \mathbf{p} + \beta m)\psi_\mu(\mathbf{p}, t), \quad (3)$$

$$\psi_{d+1}(\mathbf{p}, t) = i\alpha_i \psi_i(\mathbf{p}, t), \quad (4)$$

where $\boldsymbol{\alpha} = i\gamma_{d+1}\boldsymbol{\gamma}$ and $\beta = \gamma_{d+1}$. The constraint (4) implies that the RS fields are not just $d+1$ copies of Dirac fields. Under $\text{SO}(d)$ rotations, the time-like spinor ψ_{d+1} transforms as the $j = \frac{1}{2}$ irreducible representation, while the space-like spinors ψ_i 's (i.e. ψ_x, ψ_y, ψ_z for $d = 3$ or ψ_x, ψ_y for $d = 2$) transform as a product representation: $(j = 1) \otimes (j = \frac{1}{2})$ reducible representation which contains the irreducible ones $\phi_{3/2}(j = \frac{3}{2})$ and $\phi_{1/2}(j = \frac{1}{2})$ [49]. The details of the transformation from ψ_i 's to $\phi_{3/2}$ and

$\phi_{1/2}$ are shown in Secs. III and IV of the SM [46]. Eq. (3) is then rewritten as

$$i\partial_t \phi_{3/2}(\mathbf{p}, t) = h_{33}(\mathbf{p})\phi_{3/2}(\mathbf{p}, t) + h_{31}\phi_{1/2}(\mathbf{p}, t), \quad (5)$$

$$i\partial_t \phi_{1/2}(\mathbf{p}, t) = h_{13}(\mathbf{p})\phi_{3/2}(\mathbf{p}, t) + h_{11}\phi_{1/2}(\mathbf{p}, t), \quad (6)$$

$$i\partial_t \psi_{d+1}(\mathbf{p}, t) = H_t(\mathbf{p})\psi_{d+1}(\mathbf{p}, t), \quad (7)$$

where $H_t = \boldsymbol{\alpha} \cdot \mathbf{p} + \beta m$. The constraint equation Eq. (4) can be rewritten as the following:

$$\psi_{d+1}(\mathbf{p}, t) = R_{t1}\phi_{1/2}(\mathbf{p}, t), \quad (8)$$

with R_{t1} being a constant matrix, e.g., $R_{t1} = -i\sqrt{2}$ for $d=2$ (R_{t1} for $d=3$ is given in Sec. III of the SM [46]). Substituting Eq. (8) into Eq. (7), we obtain the Hamiltonian $H_{1/2}$ for $\phi_{1/2}$,

$$i\partial_t \phi_{1/2} = H_{1/2}\phi_{1/2}, \quad (9)$$

$$H_{1/2} = R_{t1}^{-1}H_t R_{t1}. \quad (10)$$

With Eq. (9) and (6), the relation between $\phi_{1/2}$ and $\phi_{3/2}$ is given by

$$\phi_{1/2}(\mathbf{p}, t) = R_{13}(\mathbf{p})\phi_{3/2}, \quad (11)$$

where, e.g., $R_{13} = \frac{1}{p^2+4m^2}[2mp_1 + 2mip_2\sigma_3 - i(p_1^2 - p_2^2)\sigma_2 + 2ip_1p_2\sigma_1]$ for $d = 2$. (R_{13} for $d=3$ is given in Sec. III of the SM [46].) Substituting this relation (11) into Eq. (5), we reveal the genuine Hamiltonian $H_{3/2} = h_{33} + h_{31}R_{13}$ for $\phi_{3/2}$,

$$i\partial_t \phi_{3/2}(\mathbf{p}, t) = H_{3/2}\phi_{3/2}(\mathbf{p}, t), \quad (12)$$

$$H_{3/2} = \left(m + \frac{2mp^2}{4m^2 + p^2}\right)\sigma_3 + \frac{p_1(3p_2^2 - p_1^2)}{4m^2 + p^2}\sigma_1 + \frac{p_2(p_2^2 - 3p_1^2)}{4m^2 + p^2}\sigma_2, \text{ for } d = 2; \quad (13)$$

$$H_{3/2} = \sigma_1 \otimes (\boldsymbol{\Sigma}^{\frac{3}{2}} \cdot \mathbf{p}) \left[1 + \frac{p^2 - (\boldsymbol{\Sigma}^{\frac{3}{2}} \cdot \mathbf{p})^2}{\frac{4}{9}p^2 + m^2}\right] + m\sigma_3 \otimes \left[1 + \frac{1}{2} \frac{p^2 - (\boldsymbol{\Sigma}^{\frac{3}{2}} \cdot \mathbf{p})^2}{\frac{4}{9}p^2 + m^2}\right], \text{ for } d = 3, \quad (14)$$

where $\boldsymbol{\Sigma}^{\frac{3}{2}} = \frac{2}{3}\mathbf{J}^{\frac{3}{2}}$, and $\mathbf{J}^{\frac{3}{2}}$ is angular momentum matrix in the $j = 3/2$ representation of $\text{SO}(3)$. Eq. (14) is consistent with that derived by Moldauer and Case [47] as expected.

III. CONSTRUCTION OF HAMILTONIAN FOR REALIZING RS QUASIPARTICLE IN CMS.

Suppose $\phi_{3/2}$ is the eigenvector of $H_{3/2}$ with the eigen-energy ϵ , then the components $\phi_{1/2}$ and ψ_{d+1} in the RS wave function $(\phi_{3/2}, \phi_{1/2}, \psi_{d+1})^T$ can be obtained through the constraints Eq.(11) and Eq.(8). They share

the same eigen-energy ϵ , namely,

$$H_{3/2}\phi_{3/2} = \epsilon\phi_{3/2}, \quad (15)$$

$$H_{1/2}\phi_{1/2} = \epsilon\phi_{1/2}, \quad (16)$$

$$H_t\psi_{d+1} = \epsilon\psi_{d+1}. \quad (17)$$

Therefore combining with the constraints Eq. (11) and Eq. (8), the Hamiltonian $H_{3/2}$ is sufficient for obtaining the RS wave function, and eventually the equation of motion of the RS fermion can be solved. However, this field theory approach is not operable for CM simulation because in addition to the Hamiltonian one cannot explicitly add any other equations.

In order to obtain the RS-like excitations in CMS, we propose a generic method of constructing a 16 or 6-band Hamiltonian $\bar{H}(\mathbf{p})$, which contains eigenvector Φ with components $(\Phi_{3/2}, \Phi_{1/2}, \Phi_{d+1})^T$ being exactly the same as the vector-spinor eigen wave function $(\phi_{3/2}, \phi_{1/2}, \psi_{d+1})^T$ of RS equations, with the same eigenvalue ϵ , i.e. $\bar{H}\Phi = \epsilon\Phi$, written in the following block form,

$$\begin{pmatrix} \bar{H}_{33} & \bar{H}_{31} & \bar{H}_{3t} \\ \bar{H}_{31}^\dagger & \bar{H}_{11} & \bar{H}_{1t} \\ \bar{H}_{3t}^\dagger & \bar{H}_{1t}^\dagger & \bar{H}_{tt} \end{pmatrix} \begin{pmatrix} \Phi_{3/2} \\ \Phi_{1/2} \\ \Phi_{d+1} \end{pmatrix} = \epsilon \begin{pmatrix} \Phi_{3/2} \\ \Phi_{1/2} \\ \Phi_{d+1} \end{pmatrix}. \quad (18)$$

As Φ is the same as the eigenvector of the RS equations, $\Phi_{3/2}, \Phi_{1/2}$ and Φ_{d+1} should satisfy the Eq. (15), Eq. (16) and Eq. (17), respectively, meanwhile they must also obey the RS constrains of Eq. (11) and Eq. (8). Then we can take $\bar{H}_{33} = H_{3/2}$, $\bar{H}_{11} = H_{1/2}$ and $\bar{H}_{tt} = H_t$ for the diagonal terms and demand the off-diagonal parts to satisfy the following three relations:

$$\bar{H}_{31}R_{13} + \bar{H}_{3t}R_{t1}R_{13} = 0, \quad (19)$$

$$\bar{H}_{31}^\dagger + \bar{H}_{1t}R_{t1}R_{13} = 0, \quad (20)$$

$$\bar{H}_{3t}^\dagger + \bar{H}_{1t}^\dagger R_{13} = 0. \quad (21)$$

According to Eqs. (20) and (21), \bar{H}_{31} and \bar{H}_{3t} can be expressed by \bar{H}_{1t} . Furthermore if \bar{H}_{1t} satisfies

$$R_{t1}^\dagger \bar{H}_{1t}^\dagger = -\bar{H}_{1t} R_{t1}, \quad (22)$$

the requirement namely Eq. (19) is automatically fulfilled. In high energy physics, the number of linearly independent solutions of the RS equations is exactly equal to the number of the genuine DOF, namely all of those linearly independent solutions form the basis for quantizing the RS field. However in CMS, the Hamiltonian \bar{H} has 16 (6) linearly independent eigen-solutions in 3D (2D), of which 8 (2) are identified as the emergent RS

modes while the non-RS solutions can be separated from the RS ones which is one of the merits of our method. Because of the free parameters in the off-diagonal terms of \bar{H} , we are able to tune the spectrum of the non-RS modes away from the RS ones. We will explain more details on this in the following.

Taking $d=2$ CMS for example, the general form of the off-diagonal term H_{1t} satisfying Eq. (22) reads

$$\bar{H}_{1t} = \begin{pmatrix} a_1 & b_- \\ b_+ & a_2 \end{pmatrix}, \quad (23)$$

with $b_\pm = b_1 \pm ib_2$ and $a_1, a_2, b_1, b_2 \in \mathbb{R}$ being free parameters. Once H_{1t} is given, the other off-diagonal terms \bar{H}_{13} and \bar{H}_{t3} are generated through Eq. (20) and (21), thus the Hamiltonian \bar{H} is determined. In other words, \bar{H} is parametrized by a_1, a_2, b_1 , and b_2 . We plot the spectrum of \bar{H} in Fig. 1. Two of the bands are the RS bands while the other four are the non-RS ones. They can be separated by tuning the free parameters as shown in Fig. 1. Meanwhile for any arbitrary choice of the parameters, the RS modes are unchanged with the eigen-energies and the wave functions being identical to those of the RS fermions in high energy physics.

IV. NON-RELATIVISTIC APPROXIMATION FOR HAMILTONIAN OF CMS.

With the same wave functions of RS fermion in the low-lying excitation sector, however, the Hamiltonian \bar{H} is not directly applicable to real CM materials because of its nonlocal elements arising from, say, the factor $\frac{1}{p^2+4m^2}$ in \bar{H}_{33} for $d=2$. Due to a finite mass, we make the series expansion of the nonlocal terms in \bar{H} in terms of $\frac{\mathbf{p}}{m}$. The Hamiltonian is then expanded as a 16×16 matrix for $d=3$ shown in Sec. VII of the SM [46], and 6×6 matrix for $d=2$ as follows,

$$\bar{H} \sim \begin{pmatrix} m + \frac{p^2}{2m} & 0 & -i\frac{a_1 p_-}{\sqrt{2m}} & -i\frac{b_- p_-}{\sqrt{2m}} & -\frac{a_1 p_-}{2m} & -\frac{b_- p_-}{2m} \\ 0 & -m - \frac{p^2}{2m} & -i\frac{b_+ p_+}{\sqrt{2m}} & -i\frac{a_2 p_+}{\sqrt{2m}} & -\frac{b_+ p_+}{2m} & -\frac{a_2 p_+}{2m} \\ i\frac{a_1 p_+}{\sqrt{2m}} & i\frac{b_- p_-}{\sqrt{2m}} & m & p_- & a_1 & b_- \\ i\frac{b_+ p_+}{\sqrt{2m}} & i\frac{a_2 p_-}{\sqrt{2m}} & p_+ & -m & b_+ & a_2 \\ -\frac{a_1 p_+}{2m} & -\frac{b_- p_-}{2m} & a_1 & b_- & m & p_- \\ -\frac{b_+ p_+}{2m} & -\frac{a_2 p_-}{2m} & b_+ & a_2 & p_+ & -m \end{pmatrix}. \quad (24)$$

By implementing this Hamiltonian, one can realize the 2D massive relativistic spin-3/2 RS quasiparticles in CMS. Furthermore we notice that in the non-relativistic limit, the Hamiltonian (24) can be further simplified which makes it much easier to realize in realistic CM

materials.

Up to the first order of $\frac{\mathbf{p}}{m}$, the wave functions of the

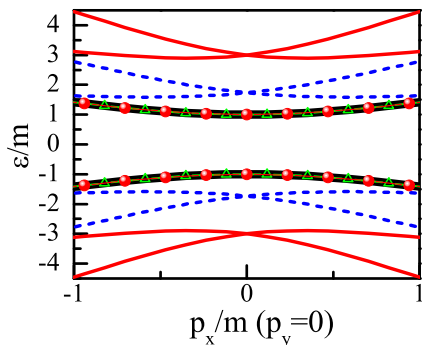


FIG. 1: For $d=2$, We plot the six bands from the \tilde{H} in Eq. (18) (namely 2D M-RS Hamiltonian in CMS). For $H_{1t} = m(\sigma_1 + \sigma_2)$, the green triangles and dashed blue lines represent the RS and non-RS modes, respectively. We also calculate the selection of $H_{1t} = 2m(\sigma_1 + \sigma_2)$, and plot the RS and non-RS modes by the red solid dots and lines, respectively. For comparison, we also show the dispersions of RS fermion by the two black thick lines. It is clear that the RS modes are exactly the same as the RS fermion, meanwhile the RS modes are separated from the non-RS modes.

RS bands read

$$\Psi_+ = (1, 0, \frac{p_x + ip_y}{2m}, 0, -i\frac{p_x + ip_y}{\sqrt{2}m}, 0)^T, \quad (25)$$

$$\Psi_- = (0, 1, 0, \frac{p_x - ip_y}{2m}, 0, -i\frac{p_x - ip_y}{\sqrt{2}m})^T, \quad (26)$$

with the corresponding eigen energies $\epsilon_{\pm} = \pm(m + \frac{p^2}{2m})$. These spectra and wave functions are exactly identical to those of the RS fermions in the non-relativistic limit. Furthermore, the positive and negative energy sectors are completely separated. Therefore the Hamiltonian in CMS can be reduced to a block diagonal form up to a unitary transformation. One is for particle while the other is for hole which are denoted as \tilde{H}_+ and \tilde{H}_- respectively. The Hamiltonians then read as[46]

$$\tilde{H}_{\pm}(\mathbf{q}) = \begin{pmatrix} \Delta_1(q_x^2 + q_y^2) & \Delta_2 q_{\mp} & \Delta_2 q_{\mp} \\ \Delta_2 q_{\pm} & \Delta_1(q_x^2 + q_y^2) + \Delta_3 & 0 \\ \Delta_2 q_{\pm} & 0 & \Delta_1(q_x^2 + q_y^2) - \Delta_3 \end{pmatrix}, \quad (27)$$

where \mathbf{p} is replaced by $\mathbf{q} = (q_x, q_y)$ which is the displacement away from a particular point in the BZ (RS point), $q_{\pm} = q_x \pm iq_y$. The real parameters Δ_1 , Δ_2 and Δ_3 can be used to construct a “light velocity” c' : $c' = |\sqrt{\frac{3}{2} \frac{\Delta_1 \Delta_3}{\Delta_2 \hbar}}|$.

To summarize this section, we shall remind that the Hamiltonian (27) effectively describes the non-relativistic 2D M-RS quasiparticles with the eigen wave functions being identical to the 2D M-RS solution to the first order of p/m . As a self-consistency check, this non-relativistic 2D M-RS quasiparticle also satisfies the RS constraints Eq. (11) and Eq. (8) to the first order of p/m . As

addressed in the next section, the non-relativistic M-RS wave function possesses a novel propertie which have not been found for spin-1/2 non-relativistic particles.

V. EXOTIC PROPERTY: FINITE ORBITAL MAGNETIZATION WITH VANISHING ORBITAL MAGNETIC MOMENT.

The non-relativistic 2D M-RS quasiparticles possesses exotic Berry-phase related properties which can be seen by solving $\tilde{H}_+(\mathbf{q})$ in Eq. (27) directly (the case of $\tilde{H}_-(\mathbf{q})$ is similar). Three eigenvalues of $\tilde{H}_+(\mathbf{q})$ are $\epsilon_{RS} = \Delta_1 q^2$ (RS band) and $\epsilon_{\pm} = \Delta_1 q^2 \pm \sqrt{\Delta_3^2 + 2\Delta_2^2 q^2}$ (non-RS bands). The corresponding eigenvectors are then, $u_{RS} = N_0(1, -\frac{\Delta_2}{\Delta_3} q_+, \frac{\Delta_2}{\Delta_3} q_+)^T$, $u_+ = N_+(\frac{2\Delta_2 q_-}{\Delta_3 + \lambda(q)}, 1, \frac{\lambda(q) - \Delta_3}{\lambda(q) + \Delta_3})^T$ and $u_- = N_-(\frac{2\Delta_2 q_-}{\Delta_3 + \lambda(q)}, -\frac{\lambda(q) - \Delta_3}{\lambda(q) + \Delta_3}, -1)^T$ where $\lambda(q) = \sqrt{\Delta_3^2 + 2\Delta_2^2 q^2}$ and N_0, N_{\pm} are the normalization factors. Calculating the Berry curvature is straightforward once we have the non-degenerate eigenvalues and eigenstates. Berry curvature behaves like a pseudo-magnetic field in the momentum space [50]. Similar to Dirac fermion, the Berry curvature of RS band, $\Omega_{RS}^z(q) = -\frac{4\Delta_2^2 \Delta_3^2}{(2\Delta_2^2 q^2 + \Delta_3^2)^2}$, is also peaked around $q=0$ point. However, with increasing value of q , it decays much faster than that of Dirac fermion [50].

Another Berry curvature related quantity is the orbital magnetic moment. They behave exactly the same under symmetry groups[50]. Arising from the self-rotating motion of the wavepacket which describes the dynamics of carriers in CMS, the orbital magnetic moment plays an important role in anomalous electronic and thermal transport properties [50, 51]. The orbital magnetic moment for a given band n is determined by $m_n^z(\mathbf{q}) = -\frac{i\epsilon}{2\hbar} (\langle \partial_{q_x} u_n | H(\mathbf{q}) - \epsilon_n(\mathbf{q}) | \partial_{q_y} u_n \rangle - c.c.)$ [52, 53]. We find that while the non-RS bands have finite orbital magnetic moments ($m_+^z(q) = -m_-^z(q) = \frac{e\Delta_2^2 \Delta_3^2}{(\Delta_3^2 + 2\Delta_2^2 q^2)^{3/2}}$), the orbital magnetic moment of the RS quasiparticle is exactly zero for an arbitrary q (i.e. $m_{RS}^z(q) = 0$). This peculiar zero result is guaranteed by the constraints on the RS fermion, not by any symmetry, because the Berry curvature is finite. As mentioned before, they transform in the same manner under symmetry groups. If this zero result of the orbital magnetic moment is dictated by symmetry, then the Berry curvature should also be zero. Although the orbital magnetic moment is exactly zero, the orbital magnetization M of the RS band is still finite due to the topological contribution coming from the Berry phase correction to the phase-space density of states for Bloch state[50, 52, 53]. Thus the non-relativistic RS band possesses a remarkable feature: Despite the nonzero orbital magnetization, under an external magnetic field there is only spin-related energy shift or splitting in the RS band spectrum. The non-relativistic RS band also provides a good platform to unambiguously clarify the unique effect from the topolog-

ical orbital magnetization[50], which usually mixes with the orbital magnetic moment thus is hard to be identified. Having the non-zero Berry curvature, finite orbital magnetization and vanishing orbital magnetic moment, the non-relativistic RS quasiparticle thus may display not only fundamental interesting physics but also peculiar properties which cannot be realized in conventional quasiparticles.

As an important physical quantity, orbital magnetic moment describes the intrinsic property of the carriers in a Bloch band. We give a criterion for the vanishing orbital magnetic moment: One can always rewrite an arbitrary $s \times s$ Hamiltonian $H_{s \times s}(q)$ ($s = 2j + 1$, j is an integer) as $H_{s \times s}(q) = h_{s \times s}(q) + C(q)I_{s \times s}$ where $C(q)$ is a scalar quantity, while $I_{s \times s}$ is a unit matrix. If the eigenvalues of $H_{s \times s}(q)$ are nondegenerate meanwhile one can find a constant unitary matrix $T_{s \times s}$, which makes $T^\dagger h_{s \times s}(q)T = -h_{s \times s}(q)$, $H_{s \times s}(q)$ should possess one band with an exactly zero orbital magnetic moment. We also give the T matrix for Eq. (27), and its existence is originated from the RS constraints (See Sec. IX of [46] for the detail).

VI. MATERIAL REALIZATIONS OF NON-RELATIVISTIC RS INSULATOR.

We now explore the possible materials to realize the non-relativistic 2D M-RS quasiparticles, i.e., the low energy $\mathbf{k} \cdot \mathbf{p}$ Hamiltonian bears the same form as \tilde{H}_\pm in Eq. (27). To realize the 3×3 matrices \tilde{H}_\pm , we consider a layered material with three layers consisting of the same atoms. Furthermore those specific atoms should comprise the identical planar structures for the three layers in order for the coefficients of the diagonal term $q_x^2 + q_y^2$ to be the same. The same coefficients also require three identical atomic orbitals to be the basis of the low energy $\mathbf{k} \cdot \mathbf{p}$ Hamiltonian. The layered structure makes the z direction different from the x and y directions in the atomic plane. Thus there is an energy splitting between p_z and $p_{x,y}$ orbitals for example. Here we take three p_z orbitals as the basis set of the low energy $\mathbf{k} \cdot \mathbf{p}$ Hamiltonian. On the other hand, from the perspective of symmetry, we firstly consider the allowable rotation symmetry operations along the z axis. The diagonal terms have the form of $q_x^2 + q_y^2$, which requires the Hamiltonian at the RS point to own C_3, C_4 or C_6 rotation symmetry[46]. The form of the off-diagonal terms $\tilde{H}_{\pm,12}$ and $\tilde{H}_{\pm,13}$ (q_\mp) (namely the coupling between different layers) rules out the possibilities of C_4 and C_6 rotation symmetry and the system belongs to either trigonal or hexagonal crystal systems which possess C_3 rotation symmetry, while the RS point should be K point (or $K' = -K, K = (1/3, 1/3)$) located at the corners of the hexagonal BZ[46]. The three layers should be of equal distances for the coefficients of q_\mp in $\tilde{H}_{\pm,12}$ and $\tilde{H}_{\pm,13}$ to be the same. Consequently the specific atoms in each layer comprise a triangular lattice which is displayed as the prototypical structure shown in

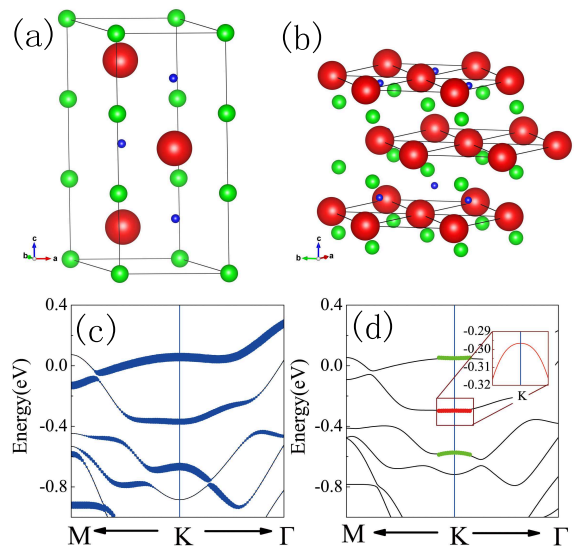


FIG. 2: (a) Crystal structure of CaLiX (X=Pb, Ge and Si): the red ones denote the X atoms, while the green ones and blue ones represent Ca atoms and Li atoms, respectively. Three X atoms form three layers, and each layer is a triangular lattice. (b) A 1-unit-cell-thick layer structure of CaLiX. (c) The electronic structure of this thin film of CaLiPb: the blue fattened curves are the projection bands for $6p_z$ orbitals of Pb. (d) The band structure of 1-unit-cell-thick layer of CaLiGe: the two green and one red thick line are the energy dispersions obtained from our low energy effective model Hamiltonian using the parameters in Table I. The red curve represents the non-relativistic 2D M-RS band.

Fig. S 1 of the SM [46]. The vanishing terms $H_{\pm,23}$ require that the hopping between the first and third layers is negligible. As seen from Eq. (27), \tilde{H}_+ or \tilde{H}_- , breaks the TR symmetry alone while they can be related to each other in the TR related \mathbf{k} points in the BZ through a TR transformation to ensure the TR symmetry of the CMS. Thus we consider the non-magnetic materials with the TR symmetry.

To our knowledge, CaLiPb is a promising candidate. CaLiPb crystallizes in the hexagonal YbAgPb type structure with space group $P\bar{6}m2$ (No. 187) [54]. The crystal structure of CaLiPb is shown as an example in Fig. 2(a), in which the three Pb atoms are located at two nonequivalent crystallographic sites: $2h(1/3, 2/3, 0.1533)$ and $1f(2/3, 1/3, 0.5)$, thus form three triangular lattices which have the same structure as the prototypical structure. Considering the energy splittings of the diagonal terms in the Hamiltonian of Eq. (27), we exfoliate CaLiPb into a 1-unit-cell-thick layer as shown in Fig. 2(b). The electronic structure of this thin film of CaLiPb is shown in Fig. 2(c). The bands of Li ions and Ca ions are far away from the Fermi level due the highly ionic property. At K point, there are considerable crystal splittings between $Pb-p_z$ and $Pb-p_x/p_y$ states as we expected. Hence, three bands near the Fermi level are

$\Delta_1(\text{eV}\cdot\text{\AA}^2)$	$\Delta_2(\text{eV}\cdot\text{\AA})$	$E_1(\text{eV})$	$E_2(\text{eV})$	$E_3(\text{eV})$	$\Delta_{23}(\text{eV})$
-1.049	-0.852	-0.296	0.049	-0.573	-0.008

TABLE I: The parameters in the Hamiltonian (28) after fitting the energy bands by first principles calculation.

mainly contributed by Pb- p_z states as shown in the fatted bands in Fig. 2(c). To avoid the large spin-orbit coupling in CaLiPb, we then consider lighter elements like Ge and Si. Fig. 2(d) shows the band structure of 2D CaLiGe which has the same lattice structure as shown in Fig. 2(b). Similar to the electronic structure of CaLiPb, three bands near the Fermi level are mainly contributed by Ge- p_z states. By fitting the energy spectrum of the following Hamiltonian (28) with that of the first-principles calculations, the parameters in the model Hamiltonian (28) can be determined.

$$\begin{pmatrix} \Delta_1(q_x^2 + q_y^2) + E_1 & & \Delta_2 q_{\pm} & & \Delta_2 q_{\pm} \\ & \Delta_2 q_{\mp} & & \Delta_1(q_x^2 + q_y^2) + E_2 & & \Delta_{23} \\ & \Delta_2 q_{\mp} & & \Delta_{23} & & \Delta_1(q_x^2 + q_y^2) + E_3 \end{pmatrix} \quad (28)$$

From the Fig. 2(d) we can see that in the vicinity of RS point, the model Hamiltonian Eq. (28) with the parameters given in Table I fits the first-principles results very well. The non-relativistic 2D M-RS mode is denoted by the red thick line in Fig. 2(d). As shown in Table I, the parameter δ_{23} is very small and can be negligible as expected. In addition to the space group $\overline{\text{P6m2}}$, there are also other eight space groups listed in Sec. X of the SM [46]. They can provide the possibilities of the similar three-layer structure as shown in Fig. 2(b), thus may also realize the non-relativistic 2D M-RS excitations.

VII. DISCUSSIONS AND CONCLUSIONS.

We studied the counterpart of spin-3/2 M-RS particles in CMS. We proposed a Hamiltonian, which implicitly contains the nontrivial constraints in RS equations and has the eigen-states exactly the same as the RS vector-spinor wave functions. Based on the perturbation method in terms of p/m , we successfully eliminated the non-local terms in the M-RS Hamiltonian, and reduced the size of the Hamiltonian matrix for 2D non-relativistic M-RS quasi fermion. We found that the orbital magnetic moment for the non-relativistic RS-band is zero while its Berry curvature and orbital magnetization are finite. We

also give a criterion, which can justify if one Hamiltonian has a zero-orbital-moment band or not. The possible lattice structures and materials were proposed. An appropriate choice of the free parameters in our proposed Hamiltonian can separate the RS bands from the non-RS bands. Furthermore, this non-relativistic RS insulator possesses TR symmetry with the TR transformation T satisfying $T^2 = 1$, thus, it fits in the AI class of the tenfold way of the classification of topological insulators[55]. Though a topologically trivial phase is expected, we believe in the non-relativistic RS insulator a finer classification exists because of the non-trivial constraints. In addition to the compounds proposed in this work, we believe by tuning these parameters (namely \vec{H}_{1t}) one can realize M-RS excitations in many different CMS.

It is worth mentioning that other higher spin relativistic particles (i.e., spin larger than 3/2) also need nontrivial constraints to project out the redundant DOF[27]. Thus the strategy we proposed for constructing the Hamiltonian for the equation of motion with constraints can also be used for the higher spin fermions and bosons such as the gravitons or any other constrained systems, and their existences and properties are possible to be explored in CMS.

Another intriguing theoretical method in dealing with constrained 2D system is the parton construction where the auxiliary gauge fields eliminate the redundant DOF[56]. Our method has the advantage of being operable while through the parton construction, we may be able to determine the fractional statistics of the 2D RS fermion which could be entirely different from the known ones because of the constraints.

Our paper provides an opportunity to study the novel properties of RS particles. Furthermore, in the presence of various types of interactions as well as the external magnetic field, this new emergent relativistic excitations in CMS may bring much more fruitful and intriguing phenomena and these study are under way.

Acknowledgments

FT acknowledges Shusheng Xu, Rui Wang and Kai Li for helpful discussions. We thank Yi Zhang for drawing our attention to the parton construction. This work was supported by the National Key R&D Program of China (No. 2017YFA0303203), NSFC under Grants No. 11525417 and No. 11374137 (FT, YPD, XGW), No. 11474061 (XL, YY).

-
- [1] P. A. M. Dirac, The quantum Theory of the Electron, *Proc. Roy. Soci. Lond. A: Math., Phys. and Eng. Sci.* **117**, 610-624 (1928).
[2] H. Weyl, Elektron und Gravitation I, *Zeitschrift Physik*

- 56**, 330-352 (1929).
[3] E. Majorana, Teoria simmetrica dell'elettrone e del positrone, *Nuovo Cimento* **14**, 171-185 (1937).
[4] A. K. Geim and K. S. Novoselov, The rise of graphene,

- Nature Materials* **6**, 183-191 (2007).
- [5] Y. Zhang, Y. W. Tan, H. L. Stormer and P. Kim, Experimental observation of the quantum Hall effect and Berry's phase in graphene, *Nature* **438**, 201-204 (2005).
- [6] M. I. Katsnelson, K. S. Novoselov and A. K. Geim, Chiral tunnelling and the Klein paradox in graphene, *Nat. Phys.* **2**, 620-625 (2006).
- [7] S. M. Young, S. Zaheer, J. C. Y. Teo, C. L. Kane, E. J. Mele, and A. M. Rappe, Dirac Semimetal in Three Dimensions, *Phys. Rev. Lett.* **108**, 140405 (2012).
- [8] Z. Wang, Y. Sun, X. Chen, C. Franchini, G. Xu, H. Weng, X. Dai, and Z. Fang, Dirac semimetal and topological phase transitions in A_3Bi ($A=Na, K, Rb$), *Phys. Rev. B* **85**, 195320 (2012).
- [9] Z. Wang, H. Weng, Q. Wu, X. Dai and Z. Fang, Three-dimensional Dirac semimetal and quantum transport in Cd_3As_2 , *Phys. Rev. B* **88**, 125427 (2013).
- [10] X. Wan, A. M. Turner, A. Vishwanath and S. Y. Savrasov Topological semimetal and Fermi-arc surface states in the electronic structure of pyrochlore iridates, *Phys. Rev. B* **83**, 205101 (2011).
- [11] L. Balents, Weyl electrons kiss, *Physics* **4**, 36 (2011).
- [12] G. B. Halász and L. Balents, Time-reversal invariant realization of the Weyl semimetal phase, *Phys. Rev. B* **85**, 035103 (2012).
- [13] H. Weng, C. Fang, Z. Fang, B. A. Bernevig and X. Dai, Weyl Semimetal Phase in Noncentrosymmetric Transition-Metal Monophosphides, *Phys. Rev. X* **5**, 011029 (2015).
- [14] S.-M. Huang, S.-Y. Xu, I. Belopolski, C.-C. Lee, G. Chang, B. Wang, N. Alidoust, G. Bian, M. Neupane, C. Zhang, S. Jia, A. Bansil, H. Lin and M. Z. Hasan, A Weyl Fermion semimetal with surface Fermi arcs in the transition metal monpnictide TaAs class, *Nat. Commun.* **6**, 7373 (2015).
- [15] A. A. Soluyanov, D. Gresch, Z. Wang, Q. Wu, M. Troyer, X. Dai and B. A. Bernevig, Type-II Weyl semimetals, *Nature* **527**, 495-498 (2015).
- [16] S.-Y. Xu, I. Belopolski, N. Alidoust, M. Neupane, G. Bian, C. Zhang, R. Sankar, G. Chang, Z. Yuan, C.-C. Lee, S.-M. Huang, H. Zheng, J. Ma, D. S. Sanchez, B. Wang, A. Bansil, F. Chou, P. P. Shibayev, H. Lin, S. Jia and M. Z. Hasan, Discovery of a Weyl fermion semimetal and topological Fermi arcs, *Science* **349**, 613-617 (2015).
- [17] B. Q. Lv, H. M. Weng, B. B. Fu, X. P. Wang, H. Miao, J. Ma, P. Richard, X. C. Huang, L. X. Zhao, G. F. Chen, Z. Fang, X. Dai, T. Qian, and H. Ding, Experimental Discovery of Weyl Semimetal TaAs, *Phys. Rev. X* **5**, 031013 (2015).
- [18] B. Q. Lv, N. Xu, H. M. Weng, J. Z. Ma, P. Richard, X. C. Huang, L. X. Zhao, G. F. Chen, C. E. Matt, F. Bisti, V. N. Strocov, J. Mesot, Z. Fang, X. Dai, T. Qian, M. Shi and H. Ding, Observation of Weyl nodes in TaAs, *Nat. Phys.* **11**, 724-727 (2015).
- [19] G. Moore and N. Read, Nonabelions in the fractional quantum hall effect, *Nucl. Phys. B* **360**, 362-396 (1991).
- [20] N. Read and D. Green, Paired states of fermions in two dimensionas with breaking of parity and time-reversal symmetries and the fractional quantum Hall effect, *Phys. Rev. B* **61**, 10267 (2000).
- [21] A. Kitaev, Unpaired Majorana fermions in quantum wires, *Phys. Usp.* **44**, 131-136 (2001).
- [22] B. I. Halperin, Quantized Hall conductance, current-carrying edge states, and the existence of extended states in a two-dimensional disordered potential, *Phys. Rev. B* **25**, 2185 (1982).
- [23] C. J. Wu, B. A. Bernevig and S. C. Zhang, Helical Liquid and the Edge of Quantum Spin Hall Systems, *Phys. Rev. Lett.* **96**, 106401 (2006).
- [24] V. Aji, Adler-Bell-Jackiw anomaly in Weyl semimetals: Application to pyrochlore iridates, *Phys. Rev. B* **85**, 241101 (2012).
- [25] D. T. Son and B. Z. Spivak, Chiral anomaly and classical negative magnetoresistance of Weyl metals, *Phys. Rev. B* **88**, 104412 (2013).
- [26] A. Kitaev, Anyons in an exactly solved model and beyond, *Ann. of Phys.* **321**, 2-111 (2006).
- [27] P. A. M. Dirac, Relativistic Wave Equations, *Proc. Roy. Soc. A* **155**, 447-459 (1936).
- [28] W. Rarita and J. Schwinger, On a Theory of Particles with Half-Integral Spin, *Phys. Rev.* **60**, 61(1941).
- [29] D. Z. Freedman and P. van Nieuwenhuizen and S. Ferrara, Progress toward a theory of supergravity, *Phys. Rev. D* **13**, 3214 (1976).
- [30] B. Bradlyn, J. Cano, Z. Wang, M. G. Vergniory, C. Felser, R. J. Cava and B. A. Bernevig, Beyond Dirac and Weyl fermions: Unconventional quasiparticles in conventional crystals, *Science* **353**, 6299 (2016).
- [31] L. Liang and Y. Yu, Semimetal with both Rarita-Schwinger-Weyl and Weyl excitations, *Phys. Rev. B* **93**, 045113 (2016).
- [32] H. Isobe and L. Fu, Quantum critical points of $j = \frac{3}{2}$ Dirac electrons in antiperovskite, *Phys. Rev. B* **93**, 241113 (2016).
- [33] M. Ezawa, Pseudospin- $\frac{3}{2}$ fermions, type-II Weyl semimetals, and critical Weyl semimetals in tricolor cubic lattices, *Phys. Rev. B* **94**, 195205 (2016).
- [34] B. Q. Lv, Z.-L. Feng, Q.-N. Xu, X. Gao, J.-Z. Ma, L.-Y. Kong, P. Richard, Y.-B. Huang, V. N. Strocov, C. Fang, H.-M. Weng, Y.-G. Shi, T. Qian and H. Ding, Observation of three-component fermions in the topological semimetal molybdenum phosphide, *Nature* **546**, 627-631 (2017).
- [35] Z. Zhu, G. W. Winkler, Q. Wu, J. Li and A. A. Soluyanov, Triple Point Topological Metals, *Phys. Rev. X* **6**, 031003 (2016).
- [36] H. Weng, C. Fang, Z. Fang and X. Dai, Coexistence of Weyl fermion and massless triply degenerate nodal points, *Phys. Rev. B* **94**, 165201 (2016).
- [37] Q. Liu, and A. Zunger, Predicted Realization of Cubic Dirac Fermion in Quasi-One-Dimensional Transition-Metal Monochalcogenides, *Phys. Rev. X* **7**, 021019 (2017).
- [38] I. C. Fulga and A. Stern, Triple point fermions in a minimal symmorphic model, *Phys. Rev. B* **95**, 241116 (2017).
- [39] Y. Xu and L.-M. Duan, Unconventional Quantum Hall Effects in Two-dimensional Triple-point Fermion Systems, arXiv.1705.05780 (2017).
- [40] G. Velo and D. Zwanziger, Propagation and Quantization of Rarita-Schwinger Waves in an External Electromagnetic Potential, *Phys. Rev.* **186**, 1337 (1969).
- [41] M. Hortaçsu, Demonstration of noncausality for the Rarita-Schwinger equation, *Phys. Rev. D* **9**, 928 (1974)
- [42] X. Luo, F. Tang, X. Wan and Y. Yu, Nonlinear Quantum Hall effects in Rarita-Schwinger gas, arXiv.1609.06956 (2016).
- [43] K. V. Klitzing, G. Dorda and M. Pepper, New Method for High-Accuracy Determination of the Fine-Structure Con-

- stant Based on Quantized Hall Resistance, *Phys. Rev. Lett.* **45**, 494 (1980).
- [44] Y. Zheng and T. Ando, Hall conductivity of a two-dimensional graphite system, *Phys. Rev. B* **65**, 245420 (2002).
- [45] G. W. Semenoff, Condensed-Matter Simulation of a Three-Dimensional Anomaly, *Phys. Rev. Lett.* **53**, 2449 (1984).
- [46] See Supplemental Material.
- [47] P. A. Moldauer and K. M. Case, Properties of Half-Integral Spin Dirac-Fierz-Pauli Particles, *Phys. Rev.* **102**, 279 (1956).
- [48] V. Bargmann and E. P. Wigner, Group Theoretical Discussion of Relativistic Wave Equations, *Proc. Nat. Acad. Sci. (USA)* **34**, 211-223 (1948).
- [49] Here j stands for either S for $d = 3$ or S^z for $d = 2$. Correspondingly, $\phi_{3/2}$ is of eight components or two-components while $\phi_{1/2}$ and ψ_{d+1} are of four or two components.
- [50] D. Xiao, M.-C. Chang and Q. Niu, Berry phase effects on electronic properties, *Rev. Mod. Phys.* **82**, 1959-2007 (2010).
- [51] X. Xu, W. Yao, D. Xiao and T. Heinz, Spin and pseudospins in layered transition metal dichalcogenides, *Nat. Phys.* **10**, 343-350 (2014).
- [52] D. Xiao, J. Shi and Q. Niu, Berry Phase Correction to Electron Density of States in Solids, *Phys. Rev. Lett.* **95**, 137204 (2005); J. Shi, G. Vignale, D. Xiao and Q. Niu, Quantum Theory of Orbital Magnetization and Its Generalization to Interacting Systems, *Phys. Rev. Lett.* **99**, 197202 (2007).
- [53] T. Thonhauser, D. Ceresoli, D. Vanderbilt and R. Resta, Orbital Magnetization in Periodic Insulators, *Phys. Rev. Lett.* **95**, 137205 (2005).
- [54] M. L. Fornasini, F. Merlo and M. Pani, Crystal structure of calcium lithium plumbide (1/1/1), *CaliPb*, and ytterbium lithium plumbide (1/1/1), *YbLiPb*, *Zeitschrift fuer Kristallographie-New Crystal Structures* **216**, 173-174 (2001).
- [55] A. P. Schnyder, S. Ryu, A. Furusaki and A. W. W. Ludwig, Classification of topological insulators and superconductors in three spatial dimensions, *Phys. Rev. B* **78**, 195125 (2008).
- [56] X. G. Wen, Projective construction of non-Abelian quantum Hall liquids, *Phys. Rev. B* **60**, 8827 (1999).

Supplemental Material

Feng Tang^{1,4,*}, Xi Luo^{2,*}, Yongping Du^{5,1,4}, Yue Yu^{3,4}, and Xiangang Wan^{1,4}

¹National Laboratory of Solid State Microstructures and School of Physics, Nanjing University, Nanjing 210093, China

²CAS Key Laboratory of Theoretical Physics, Institute of Theoretical Physics, Chinese Academy of Sciences, Beijing 100190, China

³State Key Laboratory of Surface Physics, Center for Field Theory and Particle Physics, Department of Physics, Fudan University, Shanghai 200433, China

⁴Collaborative Innovation Center of Advanced Microstructures, Nanjing 210093, China and

⁵Department of Applied Physics, Nanjing University of Science and Technology, Nanjing 210094, China

I. NOTATIONS

In quantum field theory, there are two kinds of notations for the four-vector or three-vector in 3+1 or 2+1 dimensional space-time, the imaginary time Euclidian vector $x_\mu = (\mathbf{x}, it)$ [1] or the real time Minkowski vector $x^\mu = (t, \mathbf{x})$ [2]. The Greek letters μ, ν, \dots take values from 1 to $d+1$ for the Euclidian notation and from 0 to d for the Minkowski notation. The Latin letters i, j, \dots take values from 1 to d to denote the spatial index while $d+1$ or 0 denotes the temporal index. In the Euclidian notation, we do not need to distinguish between the superscript and subscript of a vector and the metric tensor is Kronecker-delta function $\delta_{\mu\nu}$. In the Minkowski notation a contravariant vector x^μ is labeled by a superscript while a covariant vector x_μ is labeled by a subscript $x_\mu = g_{\mu\nu}x^\nu$, where the metric tensor $g_{\mu\nu} = \text{diag}(1, -1, -1, -1)$. In this work, we adopt the Euclidian notation. The vector-spinor which describes the Rarita-Schwinger (RS) field is denoted by $\psi_{\mu,\alpha}$ or ψ_μ (omitting the spinor index α). The vector spinor in the Minkowski notation can be obtained by the following substitution, $\psi_i \rightarrow \psi^i$ and $\psi_{d+1} \rightarrow i\psi^0$. Any form like $A \cdot B$ means a summation over the vector index, namely $\sum_\mu A_\mu B_\mu$. We use the units that $c = \hbar = 1$.

II. GAMMA MATRICES

We use α_i 's and β to express the γ matrices: $\gamma_i = -i\beta\alpha_i$ and $\gamma_{d+1} = \beta$ [1]. Dirac equation $(\gamma \cdot \partial + m)\psi = 0$ can be rewritten in a Hamiltonian form $i\partial_t\psi = H_D\psi$ where $H_D = \boldsymbol{\alpha} \cdot \mathbf{p} + \beta m$ [1]. In order to satisfy the relativistic energy-momentum relation, $\{\alpha_i, \alpha_j\} = 2\delta_{ij}$, $\{\alpha_i, \beta\} = 0$, $\beta^2 = 1$ and then $\{\gamma_\mu, \gamma_\nu\} = \delta_{\mu\nu}$. Hence, γ_μ are 4×4 matrices for $d = 3$ while 2×2 matrices for $d = 2$.

In three dimensional (3D) systems, we use the Dirac representation for the spinor where, $\alpha_i = \begin{pmatrix} 0 & \sigma_i \\ \sigma_i & 0 \end{pmatrix}$, and $\beta = \begin{pmatrix} \sigma_0 & 0 \\ 0 & -\sigma_0 \end{pmatrix}$. The Pauli matrices are given by $\sigma_1 = \begin{pmatrix} 0 & 1 \\ 1 & 0 \end{pmatrix}$, $\sigma_2 = \begin{pmatrix} 0 & -i \\ i & 0 \end{pmatrix}$, and $\sigma_3 = \begin{pmatrix} 1 & 0 \\ 0 & -1 \end{pmatrix}$. $\sigma_0 = I_{2 \times 2}$ is the identity matrix. In this representation, for the rest coordinate frame (i.e., $\mathbf{p} = (0, 0, 0)$), the Dirac Hamiltonian is already diagonalized: $\text{diag}(m, m, -m, -m)$, and one can denote the spinor index as $(\xi\sigma)$ where $\xi = \pm$ and $\sigma = \uparrow, \downarrow$. In the Weyl representation, the representation of the Lorentz group is $(\frac{1}{2}, 0) \oplus (0, \frac{1}{2})$ [2]. The spinor index is denoted by $(\zeta\sigma)$ where $\zeta = L, R$ and $\sigma = \uparrow, \downarrow$. The spinors in the Dirac representation are related to the spinors in the Weyl representation by $\psi_{+,\sigma} = \frac{1}{\sqrt{2}}(\psi_{L,\sigma} - \psi_{R,\sigma})$, $\psi_{-,\sigma} = \frac{1}{\sqrt{2}}(\psi_{L,\sigma} + \psi_{R,\sigma})$. We use the Dirac representation in this work. In two dimensional (2D) systems (located in the xy plane) where p_3 is set to be zero, it is convenient to use three Pauli matrices to represent α_1, α_2 and β , and we can choose $\alpha_1 = \sigma_1$, $\alpha_2 = \sigma_2$ and $\beta = \sigma_3$. We will discuss the dimensional reduction from $d = 3$ to $d = 2$ in Sec. V.

*These two authors contribute equally.

III. 3D RS HAMILTONIANS

In this section, we derive the 3D RS Hamiltonians. We define $\Sigma^{\frac{3}{2}} = \frac{2}{3}\mathbf{J}^{\frac{3}{2}}$ where $\mathbf{J}^{\frac{3}{2}}$ are 4×4 vector matrices of the angular momentum operator in the representation $j = \frac{3}{2}$ of SO(3) group with the following basis set:

$$|\frac{3}{2}, \frac{3}{2}\rangle, |\frac{3}{2}, -\frac{3}{2}\rangle, |\frac{3}{2}, \frac{1}{2}\rangle, |\frac{3}{2}, -\frac{1}{2}\rangle$$

. Namely,

$$J_1^{\frac{3}{2}} = \begin{pmatrix} 0 & 0 & \frac{\sqrt{3}}{2} & 0 \\ 0 & 0 & 0 & \frac{\sqrt{3}}{2} \\ \frac{\sqrt{3}}{2} & 0 & 0 & 1 \\ 0 & \frac{\sqrt{3}}{2} & 1 & 0 \end{pmatrix},$$

$$J_2^{\frac{3}{2}} = \begin{pmatrix} 0 & 0 & -i\frac{\sqrt{3}}{2} & 0 \\ 0 & 0 & 0 & i\frac{\sqrt{3}}{2} \\ i\frac{\sqrt{3}}{2} & 0 & 0 & -i \\ 0 & -i\frac{\sqrt{3}}{2} & i & 0 \end{pmatrix},$$

$$J_3^{\frac{3}{2}} = \begin{pmatrix} \frac{3}{2} & 0 & 0 & 0 \\ 0 & -\frac{3}{2} & 0 & 0 \\ 0 & 0 & \frac{1}{2} & 0 \\ 0 & 0 & 0 & -\frac{1}{2} \end{pmatrix}.$$

The space-like spinors ψ_1, ψ_2, ψ_3 (or ψ_x, ψ_y, ψ_z) are a product representation $1 \otimes \frac{1}{2}$ of SO(3) group. They are related to the $j = \frac{3}{2}$ and $j = \frac{1}{2}$ irreducible representations by

$$\begin{pmatrix} \psi_{1,\xi,\uparrow} \\ \psi_{1,\xi,\downarrow} \\ \psi_{2,\xi,\uparrow} \\ \psi_{2,\xi,\downarrow} \\ \psi_{3,\xi,\uparrow} \\ \psi_{3,\xi,\downarrow} \end{pmatrix} = \begin{pmatrix} -\frac{1}{\sqrt{2}} & 0 & 0 & \frac{1}{\sqrt{6}} & 0 & -\frac{1}{\sqrt{3}} \\ 0 & \frac{1}{\sqrt{2}} & -\frac{1}{\sqrt{6}} & 0 & -\frac{1}{\sqrt{3}} & 0 \\ -\frac{i}{\sqrt{2}} & 0 & 0 & -\frac{i}{\sqrt{6}} & 0 & \frac{i}{\sqrt{3}} \\ 0 & -\frac{i}{\sqrt{2}} & -\frac{i}{\sqrt{6}} & 0 & -\frac{i}{\sqrt{3}} & 0 \\ 0 & 0 & \sqrt{\frac{2}{3}} & 0 & -\frac{1}{\sqrt{3}} & 0 \\ 0 & 0 & 0 & \sqrt{\frac{2}{3}} & 0 & \frac{1}{\sqrt{3}} \end{pmatrix} \begin{pmatrix} \phi_{\xi, \frac{3}{2}, -\frac{3}{2}} \\ \phi_{\xi, \frac{3}{2}, -\frac{3}{2}} \\ \phi_{\xi, \frac{3}{2}, \frac{1}{2}} \\ \phi_{\xi, \frac{3}{2}, -\frac{1}{2}} \\ \phi_{\xi, \frac{1}{2}, \frac{1}{2}} \\ \phi_{\xi, \frac{1}{2}, -\frac{1}{2}} \end{pmatrix} \equiv R \begin{pmatrix} \phi_{\xi, \frac{3}{2}, -\frac{3}{2}} \\ \phi_{\xi, \frac{3}{2}, -\frac{3}{2}} \\ \phi_{\xi, \frac{3}{2}, \frac{1}{2}} \\ \phi_{\xi, \frac{3}{2}, -\frac{1}{2}} \\ \phi_{\xi, \frac{1}{2}, \frac{1}{2}} \\ \phi_{\xi, \frac{1}{2}, -\frac{1}{2}} \end{pmatrix}. \quad (1)$$

In $\phi_{\xi, \frac{3}{2}, \frac{3}{2}}$, the first $\frac{3}{2}$ represents j and the second represents j_z . We use $\phi_{\xi, \frac{3}{2}}$ to represent $(\phi_{\xi, \frac{3}{2}, \frac{3}{2}}, \phi_{\xi, \frac{3}{2}, -\frac{3}{2}}, \phi_{\xi, \frac{3}{2}, \frac{1}{2}}, \phi_{\xi, \frac{3}{2}, -\frac{1}{2}})^T$, and $\phi_{\xi, \frac{1}{2}}$ to represent $(\phi_{\xi, \frac{1}{2}, \frac{1}{2}}, \phi_{\xi, \frac{1}{2}, -\frac{1}{2}})^T$. According to $(\gamma \cdot \partial + m)\psi_i = 0$ or $i\partial_t\psi_i = H_D\psi_i$ in the RS equations, we get the equations of motion of $\phi_{\xi, \frac{3}{2}}$ and $\phi_{\xi, \frac{1}{2}}$:

$$i\partial_t\phi_{\xi, \frac{3}{2}} = h'_{33}(\mathbf{p})\phi_{\xi, \frac{3}{2}} + h'_{31}(\mathbf{p})\phi_{\xi, \frac{1}{2}} + \xi m\phi_{\xi, \frac{3}{2}}, \quad (2)$$

$$i\partial_t\phi_{\xi, \frac{1}{2}} = h'_{13}(\mathbf{p})\phi_{\xi, \frac{3}{2}} + h'_{11}(\mathbf{p})\phi_{\xi, \frac{1}{2}} + \xi m\phi_{\xi, \frac{1}{2}}, \quad (3)$$

where $h' = R^\dagger(I_{3 \times 3} \otimes \boldsymbol{\sigma} \cdot \mathbf{p})R$. Namely,

$$h'(\mathbf{p}) = \begin{pmatrix} h'_{33} & h'_{31} \\ h'_{13} & h'_{11} \end{pmatrix}, \quad (4)$$

where $h'_{33} = \mathbf{p} \cdot \Sigma^{\frac{3}{2}}$, $h'_{11} = -\frac{1}{3}\mathbf{p} \cdot \boldsymbol{\sigma}$, and $h'_{31} = h'^{\dagger}_{13} = \begin{pmatrix} \sqrt{\frac{2}{3}}p_- & 0 \\ 0 & -\sqrt{\frac{2}{3}}p_+ \\ -\frac{2\sqrt{2}}{3}p_3 & \frac{\sqrt{2}}{3}p_- \\ -\frac{\sqrt{2}}{3}p_+ & -\frac{2\sqrt{2}}{3}p_3 \end{pmatrix}$, with $p_- = p_+^* = p_1 - ip_2$.

Simultaneously the constraints $\gamma \cdot \psi = 0$ in the RS equations become

$$\psi_{4,\xi} = -i\sqrt{3}\phi_{\xi,\frac{1}{2}}. \quad (5)$$

Substituting this equation into $(\gamma \cdot \partial + m)\psi_4 = 0$ or $i\partial_t\psi_4 = H_D\psi_4$, we get

$$i\partial_t\phi_{\xi,\frac{1}{2}} = \boldsymbol{\sigma} \cdot \mathbf{p}\phi_{\xi,\frac{1}{2}} - \xi m\phi_{\xi,\frac{1}{2}}. \quad (6)$$

As we will show later, Eq. (2) and Eq. (3) correspond to Eq. (5) and Eq. (6) in the main text, respectively; Eq. (5) and Eq. (6) correspond to Eq. (8) and Eq. (9) in the main text, respectively. Combining Eq. (6) and Eq. (3), we get the relation between $\phi_{\xi,\frac{3}{2}}$ and $\phi_{\xi,\frac{1}{2}}$:

$$h'_{13}\phi_{\xi,\frac{3}{2}} + 4h'_{11}\phi_{\xi,\frac{1}{2}} = 2m\xi\phi_{\xi,\frac{1}{2}}, \quad (7)$$

from which we have

$$\phi_{\xi,\frac{1}{2}} = (m^2 + 4h'^2_{11})^{-1}(-h'_{11}h'_{13}\phi_{\xi,\frac{3}{2}} + \xi\frac{m}{2}h'_{13}\phi_{\xi,\frac{3}{2}}), \quad (8)$$

which corresponds to Eq. (11) in the main text. It is clear that $\phi_{\xi,\frac{1}{2}}$ and $\psi_{4,\xi}$ are indeed redundant degrees of freedom (DOF) and can be obtained from genuine DOF $\phi_{\xi,\frac{3}{2}}$ with Eq. (5) and Eq. (8). By substituting Eq. (8) into Eq. (2), we find that the Hamiltonian of $\phi_{\xi,\frac{3}{2}}$,

$$i\partial_t\phi_{\xi,\frac{3}{2}} = (h'_{33} - (m^2 + 4h'^2_{11})^{-1}h'_{31}h'_{11}h'_{13})\phi_{\xi,\frac{3}{2}} + \xi m(1 + \frac{1}{2}(m^2 + 4h'^2_{11})^{-1}h'_{31}h'_{13})\phi_{\xi,\frac{3}{2}}. \quad (9)$$

Notice that $h'^2_{11} = \frac{1}{9}p^2$, $-h'_{31}h'_{11}h'_{13} = (\boldsymbol{\Sigma}^{\frac{3}{2}} \cdot \mathbf{p})(p^2 - (\boldsymbol{\Sigma}^{\frac{3}{2}} \cdot \mathbf{p})^2)$, and $h'_{31}h'_{13} = p^2 - (\boldsymbol{\Sigma}^{\frac{3}{2}} \cdot \mathbf{p})^2$. We can then write the above equation in a more compact form:

$$i\frac{\partial}{\partial t}\phi_{\xi,\frac{3}{2}} = \boldsymbol{\Sigma}^{\frac{3}{2}} \cdot \mathbf{p}[1 + \frac{p^2 - (\boldsymbol{\Sigma}^{\frac{3}{2}} \cdot \mathbf{p})^2}{\frac{4}{9}p^2 + m^2}]\phi_{\xi,\frac{3}{2}} + \xi m[1 + \frac{1}{2}\frac{p^2 - (\boldsymbol{\Sigma}^{\frac{3}{2}} \cdot \mathbf{p})^2}{\frac{4}{9}p^2 + m^2}]\phi_{\xi,\frac{3}{2}}. \quad (10)$$

If we represent $(\phi_{+,\frac{3}{2}}, \phi_{-,\frac{3}{2}})^T$ by $\phi_{3/2}$, and $(\phi_{+,\frac{1}{2}}, \phi_{-,\frac{1}{2}})^T$ by $\phi_{1/2}$, (5) and (8) can be written in the following form

$$\psi_4 = -i\sqrt{3}\sigma_1 \otimes \sigma_0\phi_1 \equiv R_{t1}\phi_{1/2}, \quad (11)$$

$$\phi_{1/2} = \frac{1}{\frac{4}{9}p^2 + m^2}(-\sigma_0 \otimes h'_{11}h'_{13} + \frac{m}{2}i\sigma_2 \otimes h'_{13})\phi_{3/2} \equiv R_{13}\phi_{3/2}. \quad (12)$$

Eq. (2), Eq. (3) and Eq. (6) can be written in the following compact form:

$$i\partial_t\phi_{3/2} = h_{33}\phi_3 + h_{31}\phi_{1/2}, \quad (13)$$

$$i\partial_t\phi_{1/2} = h_{13}\phi_3 + h_{11}\phi_{1/2}, \quad (14)$$

$$i\partial_t\phi_{1/2} = H_{1/2}\phi_{1/2}, \quad (15)$$

where, $h_{33} = \begin{pmatrix} m & h'_{33} \\ h'_{33} & -m \end{pmatrix}$, $h_{31} = \begin{pmatrix} 0 & h'_{31} \\ h'_{31} & 0 \end{pmatrix}$, $h_{11} = \begin{pmatrix} m & h'_{11} \\ h'_{11} & -m \end{pmatrix}$ and $H_{1/2} = \boldsymbol{\alpha} \cdot \mathbf{p} - \beta m = R_{t1}^{-1}H_tR_{t1}$. Eq. (10) can also be written as,

$$i\partial_t\phi_{3/2} = H_{3/2}\phi_{3/2}, \quad (16)$$

where $H_{3/2} = \sigma_1 \otimes (\boldsymbol{\Sigma}^{\frac{3}{2}} \cdot \mathbf{p})[1 + \frac{p^2 - (\boldsymbol{\Sigma}^{\frac{3}{2}} \cdot \mathbf{p})^2}{\frac{4}{9}p^2 + m^2}] + m\sigma_3 \otimes [1 + \frac{1}{2}\frac{p^2 - (\boldsymbol{\Sigma}^{\frac{3}{2}} \cdot \mathbf{p})^2}{\frac{4}{9}p^2 + m^2}]$.

IV. 2D RS HAMILTONIANS

The situation for the 2D RS systems is similar to that in the 3D RS systems. In the 2D systems, the typical elements of the Lorentz group would be just the boosts along the x - and y -directions as well as the pure rotations around the z -axis. The pure rotation group is then $SO(2)$. To characterize the angular momentum we merely need one number j_z instead of (j, j_z) in the 3D systems. In the 2D systems, the vector spinor field would be explicitly written as follows for the sake of clarity: $\psi_1(\mathbf{x}, t) = \begin{pmatrix} \psi_1(\mathbf{x}, t, \uparrow) \\ \psi_1(\mathbf{x}, t, \downarrow) \end{pmatrix}$, $\psi_2(\mathbf{x}, t) = \begin{pmatrix} \psi_2(\mathbf{x}, t, \uparrow) \\ \psi_2(\mathbf{x}, t, \downarrow) \end{pmatrix}$, $\psi_3(\mathbf{x}, t) = \begin{pmatrix} \psi_3(\mathbf{x}, t, \uparrow) \\ \psi_3(\mathbf{x}, t, \downarrow) \end{pmatrix}$, where ψ_1, ψ_2 (or ψ_x, ψ_y) are space-like spinors while ψ_3 is a time-like spinor. In the momentum representation, the RS equations would be written as follows:

$$i\partial_t\psi_1(\mathbf{p}, t) = (\boldsymbol{\sigma} \cdot \mathbf{p} + m\sigma_3)\psi_1(\mathbf{p}, t), \quad (17)$$

$$i\partial_t\psi_2(\mathbf{p}, t) = (\boldsymbol{\sigma} \cdot \mathbf{p} + m\sigma_3)\psi_2(\mathbf{p}, t), \quad (18)$$

$$i\partial_t\psi_3(\mathbf{p}, t) = (\boldsymbol{\sigma} \cdot \mathbf{p} + m\sigma_3)\psi_3(\mathbf{p}, t), \quad (19)$$

with the constraint: $\psi_3(\mathbf{p}, t) = i\sigma_i\psi_i(\mathbf{p}, t)$.

We would make the following unitary transformation in order to extract the genuine DOF which are in the space of $j_z = \pm\frac{3}{2}$ representations of $SO(2)$:

$$\begin{pmatrix} \psi_{1,\uparrow} \\ \psi_{1,\downarrow} \\ \psi_{2,\uparrow} \\ \psi_{2,\downarrow} \end{pmatrix} = \begin{pmatrix} -\frac{1}{\sqrt{2}} & 0 & 0 & -\frac{1}{\sqrt{2}} \\ 0 & \frac{1}{\sqrt{2}} & -\frac{1}{\sqrt{2}} & 0 \\ -\frac{i}{\sqrt{2}} & 0 & 0 & \frac{i}{\sqrt{2}} \\ 0 & -\frac{i}{\sqrt{2}} & -\frac{i}{\sqrt{2}} & 0 \end{pmatrix} \begin{pmatrix} \phi_{j_z=\frac{3}{2}} \\ \phi_{j_z=-\frac{3}{2}} \\ \phi_{j_z=\frac{1}{2}} \\ \phi_{j_z=-\frac{1}{2}} \end{pmatrix}, \quad (20)$$

where $\phi_{j_z=\pm\frac{3}{2}, \pm\frac{1}{2}}$ transform as j_z representation under $SO(2)$. We can easily transform (17) and (18) into the above new representation. Denoting $(\phi_{j_z=\frac{3}{2}}, \phi_{j_z=-\frac{3}{2}})^T$ as $\phi_{3/2}$ and $(\phi_{j_z=\frac{1}{2}}, \phi_{j_z=-\frac{1}{2}})^T$ as $\phi_{1/2}$:

$$i\partial_t\phi_{3/2} = h_{33}\phi_{3/2} + h_{31}\phi_{1/2}, \quad (21)$$

$$i\partial_t\phi_{1/2} = h_{13}\phi_{3/2} + h_{11}\phi_{1/2}, \quad (22)$$

where

$$h_{33} = h_{11} = -\sigma_3 m, h_{31} = h_{13}^\dagger = \text{diag}(p_-, -p_+), \quad (23)$$

and the constraint (19) would be,

$$\psi_3 = -i\sqrt{2}\phi_{1/2} \equiv R_{t1}\phi_{1/2}. \quad (24)$$

As (19) describes the equation of motion of ψ_3 , its Hamiltonian H_t is given by

$$H_t = \boldsymbol{\alpha} \cdot \mathbf{p} + \sigma_3 m. \quad (25)$$

Substituting (24) into (19) we will get the Hamiltonian of ϕ_1 ,

$$i\partial_t\phi_{1/2} = H_{1/2}\phi_{1/2}, \quad (26)$$

where $H_{1/2} = R_{t1}^{-1}H_t R_{t1} = \boldsymbol{\sigma} \cdot \mathbf{p} + \sigma_3 m$. Combining (22) and (26), we get,

$$\phi_{1/2} = \frac{1}{4m^2 + p^2} \begin{pmatrix} 2mp_+ & -p_-^2 \\ p_+^2 & 2mp_- \end{pmatrix} \phi_{3/2} \equiv R_{13}\phi_{3/2}. \quad (27)$$

Substituting (27) into (21), we have

$$i\partial_t\phi_{3/2} = H_{3/2}\phi_{3/2}, \quad (28)$$

where $H_{3/2} = \begin{pmatrix} m + \frac{2mp^2}{4m^2+p^2} & -\frac{p_-^3}{4m^2+p^2} \\ -\frac{p_+^3}{4m^2+p^2} & -(m + \frac{2mp^2}{4m^2+p^2}) \end{pmatrix}$. Notice that when setting $p_3 = 0$ and $\psi_3 = (0, 0, 0, 0)^T$ in three dimensions, the results in the 3D RS systems will turn into those of the 2D RS systems.

V. FROM $d = 3$ TO $d = 2$

For the Dirac field, when the spatial dimension is reduced from three to two and the 2D system is located in the xy plane, we can set $p_3 = 0$. We use the superscripts $3D$ or $2D$ to distinguish between the quantities in 3D or 2D. It is easy to find that H_D^{3D} can be written in a block-diagonalized form when we write the wave function as $(\psi_{+, \uparrow}^{3D}, \psi_{-, \downarrow}^{3D}, \psi_{-, \uparrow}^{3D}, \psi_{+, \downarrow}^{3D})^T$:

$$H_D^{3D} = \begin{pmatrix} m & p_- & 0 & 0 \\ p_+ & -m & 0 & 0 \\ 0 & 0 & -m & p_- \\ 0 & 0 & p_+ & m \end{pmatrix}. \quad (29)$$

Then the 3D Dirac equation will be reduced to two 2D Dirac equations with masses of opposite signs, i.e. $\pm m$. If we define $\psi_{\uparrow}^{2D, m} = \psi_{+, \uparrow}^{3D}$, $\psi_{\downarrow}^{2D, m} = \psi_{-, \downarrow}^{3D}$ and $\psi_{\uparrow}^{2D, -m} = \psi_{-, \uparrow}^{3D}$, $\psi_{\downarrow}^{2D, -m} = \psi_{+, \downarrow}^{3D}$, then the two 2D Dirac equations would be, $i\partial_t \psi^{2D, \pm m} = (\sigma_1 p_1 + \sigma_2 p_2 \pm \sigma_3 m) \psi^{2D, \pm m}$.

As for the RS field, we will show how the 3D RS vector spinor can be reduced to two 2D RS vector spinors by setting $p_3 = 0$ and $\psi_3^{3D} = (0, 0, 0, 0)^T$. Analogously as the Dirac field, we expect that by setting $\psi_{i, \uparrow}^{2D, m} = \psi_{i, \uparrow}^{3D}$, $\psi_{i, \downarrow}^{2D, m} = \psi_{i, \downarrow}^{3D}$ and $\psi_{i, \uparrow}^{2D, -m} = \psi_{i, -\uparrow}^{3D}$, $\psi_{i, \downarrow}^{2D, -m} = \psi_{i, +\downarrow}^{3D}$ with $i = 1, 2$, the Dirac equations for ψ_i^{3D} will change to two decoupled 2D Dirac equations with masses of opposite signs, i.e., $i\partial_t \psi_i^{2D, \pm m} = (\sigma_1 p_1 + \sigma_2 p_2 \pm \sigma_3 m) \psi_i^{2D, \pm m}$. For the constraint,

$$\gamma^{3D} \cdot \psi^{3D} = 0, \text{ i.e., } \psi_4^{3D} = i\alpha_1^{3D} \psi_1^{3D} + i\alpha_2^{3D} \psi_2^{3D}, \text{ then } \begin{pmatrix} \psi_{4, +, \uparrow} \\ \psi_{4, +, \downarrow} \\ \psi_{4, -, \uparrow} \\ \psi_{4, -, \downarrow} \end{pmatrix} = i \begin{pmatrix} \psi_{1, -, \downarrow} - i\psi_{2, -, \downarrow} \\ \psi_{1, -, \uparrow} + i\psi_{2, -, \uparrow} \\ \psi_{1, +, \downarrow} - i\psi_{2, +, \downarrow} \\ \psi_{1, +, \uparrow} + i\psi_{2, +, \uparrow} \end{pmatrix}. \text{ We can find that,}$$

$\begin{pmatrix} \psi_{4, +, \uparrow}^{3D} \\ \psi_{4, -, \downarrow}^{3D} \end{pmatrix} = i \begin{pmatrix} \psi_{1, -, \downarrow}^{3D} - i\psi_{2, -, \downarrow}^{3D} \\ \psi_{1, +, \uparrow}^{3D} + i\psi_{2, +, \uparrow}^{3D} \end{pmatrix}$, and $\begin{pmatrix} \psi_{4, -, \uparrow}^{3D} \\ \psi_{4, +, \downarrow}^{3D} \end{pmatrix} = i \begin{pmatrix} \psi_{1, +, \downarrow}^{3D} - i\psi_{2, +, \downarrow}^{3D} \\ \psi_{1, -, \uparrow}^{3D} + i\psi_{2, -, \uparrow}^{3D} \end{pmatrix}$. By setting $\psi_{3, \uparrow}^{2D, m} = \psi_{4, +, \uparrow}^{3D}$, $\psi_{3, \downarrow}^{2D, m} = \psi_{4, -, \downarrow}^{3D}$, and $\psi_{3, \uparrow}^{2D, -m} = \psi_{4, -, \uparrow}^{3D}$, $\psi_{3, \downarrow}^{2D, -m} = \psi_{4, +, \downarrow}^{3D}$, we can find that for both $\psi_3^{2D, m}$ and $\psi_3^{2D, -m}$, they satisfy $\psi_3^{2D, \pm m} = i\sigma_1 \psi_1^{2D, \pm m} + i\sigma_2 \psi_2^{2D, \pm m}$, i.e., $\gamma^{2D} \cdot \psi^{2D, \pm m} = 0$. Furthermore the time-like spinors in 2D: $\psi_3^{2D, \pm m}$ also satisfy the 2D Dirac equations: $i\partial_t \psi_3^{2D, \pm m} = (\sigma_1 p_1 + \sigma_2 p_2 \pm \sigma_3 m) \psi_3^{2D, \pm m}$.

In summary, the 3D RS equations are reduced to two sets of 2D RS equations with masses $\pm m$: $i\partial_t \psi_\mu^{2D, \pm m} = (\sigma_1 p_1 + \sigma_2 p_2 \pm \sigma_3 m) \psi_\mu^{2D, \pm m}$ with a nontrivial constraint $\gamma^{2D} \cdot \psi^{2D, \pm m} = 0$ after setting $p_3 = 0$ and $\psi_3^{3D} = (0, 0, 0, 0)^T$. According to the transformations in (1) and (20) and using the above relations between the vector spinors in 3D and 2D, it is easy to get (keeping in mind that $\psi_3^{3D} = (0, 0, 0, 0)^T$),

$$\phi_{\xi, \frac{3}{2}, \frac{3}{2}}^{3D} = \phi_{\frac{3}{2}}^{2D, \xi m}, \quad (30)$$

$$\phi_{\xi, \frac{3}{2}, -\frac{3}{2}}^{3D} = \phi_{-\frac{3}{2}}^{2D, \xi m}, \quad (31)$$

$$\phi_{\xi, \frac{3}{2}, \frac{1}{2}}^{3D} = \frac{1}{\sqrt{2}} \phi_{\xi, \frac{1}{2}, \frac{1}{2}}^{3D} = \frac{1}{\sqrt{3}} \phi_{\frac{1}{2}}^{2D, \xi m} \quad (32)$$

$$\phi_{\xi, \frac{3}{2}, -\frac{1}{2}}^{3D} = -\frac{1}{\sqrt{2}} \phi_{\xi, \frac{1}{2}, -\frac{1}{2}}^{3D} = -\frac{1}{\sqrt{3}} \phi_{-\frac{1}{2}}^{2D, \xi m}. \quad (33)$$

Because $\phi_{\xi, \frac{3}{2}, \pm \frac{1}{2}}^{3D}$ and $\phi_{\xi, \frac{1}{2}, \pm \frac{1}{2}}^{3D}$ are the same representations for $SO(2)$ group, they differ just by a constant. Using the above equations, we have checked that the 3D results in Sec. III will recover those of 2D in Sec. IV.

VI. THE SELECTION OF \bar{H}_{1t}

In addition to the RS modes, the Hamiltonian in condensed matter systems (CMS) (i.e., the \bar{H} in the Eq. (18) in the main text) contains the other non-RS modes. Since we are only interested in the dispersion of the RS modes, as shown in the main text, the only requirement for \bar{H}_{1t} is $R_{t1}^\dagger \bar{H}_{1t}^\dagger + \bar{H}_{1t} R_{t1} = 0$, which cannot fully determine the expression of \bar{H}_{1t} . For $d = 2$, $R_{t1} = -i\sqrt{2}$, thus $\bar{H}_{1t}^\dagger = \bar{H}_{1t}$, and \bar{H}_{1t} has the following form,

$$\bar{H}_{1t} = \begin{pmatrix} a_1 & b_- \\ b_+ & a_2 \end{pmatrix}, \quad (34)$$

where $b_{\pm} = b_1 \pm ib_2$ and a_1, a_2, b_1, b_2 are independent real parameters. We plot the band spectrum with $\bar{H}_{1t} = m(\sigma_1 + \sigma_2)$ (i.e., $a_1 = a_2 = 0, b_1 = b_2 = m$) in Fig. 1 of the main text. It is clear that the RS modes are separated from the non-RS modes. We also plot the bands for another selection of $a_1 = a_2 = 0, b_1 = b_2 = 2m$. It is clear that with changing \bar{H}_{1t} by the restriction of $R_{t1}^\dagger \bar{H}_{1t}^\dagger + \bar{H}_{1t} R_{t1} = 0$, the RS modes will not be modified, i.e., they are protected from such a change, while the non-RS modes will be modified. And once $\bar{H}_{1t} \neq \begin{pmatrix} 0 & 0 \\ 0 & 0 \end{pmatrix}$, the non-RS and RS modes are separated.

For $d = 3$, $\bar{H}_{1t}^\dagger = (\sigma_1 \otimes \sigma_0) \bar{H}_{1t} (\sigma_1 \otimes \sigma_0)$, then, if we write \bar{H}_{1t} in a blocking form,

$$\bar{H}_{1t} = \begin{pmatrix} \bar{H}_{1t,++} & \bar{H}_{1t,+ -} \\ \bar{H}_{1t,- +} & \bar{H}_{1t,--} \end{pmatrix}, \quad (35)$$

where $\bar{H}_{1t, \xi \xi'}(\xi, \xi' = +/ -)$ is a 2×2 matrix, we will find $\bar{H}_{1t, --} = \bar{H}_{1t, ++}^\dagger$, $\bar{H}_{1t, + -} = \bar{H}_{1t, + -}^\dagger$ and $\bar{H}_{1t, - +} = \bar{H}_{1t, - +}^\dagger$. We then find that,

$$\bar{H}_{1t, ++} = \begin{pmatrix} a_+ & b_+ \\ c_+ & d_+ \end{pmatrix}, \bar{H}_{1t, --} = \bar{H}_{1t, ++}^\dagger, \quad (36)$$

$$\bar{H}_{1t, + -} = \begin{pmatrix} e_1 & f_- \\ f_+ & e_2 \end{pmatrix}, \bar{H}_{1t, - +} = \begin{pmatrix} g_1 & h_- \\ h_+ & g_2 \end{pmatrix}. \quad (37)$$

where $a_+ = a_1 + ia_2, b_+ = b_1 + ib_2, c_+ = c_1 + ic_2, d_+ = d_1 + id_2, f_{\pm} = f_1 \pm if_2, h_{\pm} = h_1 \pm ih_2$ and $a_1, a_2, b_1, b_2, c_1, c_2, d_1, d_2, e_1, e_2, f_1, f_2, g_1, g_2, h_1, h_2$ are all real parameters. In order to separate the RS modes from the other non-RS modes, we should choose appropriate parameters, i.e., \bar{H}_{1t} can't be a zero matrix. This guarantees that the low energy physics can exhibit the RS physics.

VII. EXPANSION FOR HAMILTONIAN

As stated in the main text, we can directly expand the nonlocal elements in $\bar{H}(\mathbf{p})$, i.e., expanding $H_{3/2}, R_{13}$ as the series of $\frac{\mathbf{p}}{m}$. For $d = 3$,

$$R_{13} = \begin{pmatrix} 0 & \frac{h'_{13}}{2m} \\ \frac{h'_{13}}{2m} & 0 \end{pmatrix} + O\left(\frac{p^2}{m^2}\right), \quad (38)$$

$$H_{3/2} = \sigma_1 \otimes \Sigma^{\frac{3}{2}} \cdot \mathbf{p} + m\sigma_3 \otimes \sigma_0 + O\left(\frac{p^2}{m^2}\right). \quad (39)$$

For $d = 2$,

$$R_{13} = \begin{pmatrix} \frac{p_+}{2m} & 0 \\ 0 & \frac{p_-}{2m} \end{pmatrix} + O\left(\frac{p^2}{m^2}\right), \quad (40)$$

$$H_{3/2} = \begin{pmatrix} m + \frac{p^2}{2m} & 0 \\ 0 & -m - \frac{p^2}{2m} \end{pmatrix} + O\left(\frac{p^4}{m^4}\right). \quad (41)$$

The Hamiltonians for $\phi_{1/2}$ and ψ_{d+1} take the original form because they contain no nonlocal terms. For $d = 3$ or $d = 2$, we have given the form of H_{1t} in Sec. VI. According to the main text, $\bar{H}_{13} = -\bar{H}_{1t} R_{t1} R_{13}$ and $\bar{H}_{t3} = -\bar{H}_{t1} R_{13}$. Because \bar{H} is Hermitian, we can then get the expansions of all the block matrices. Although without nonlocal terms, the Hamiltonian matrix in CMS is still very large (6×6 for $d = 2$ while 16×16 for $d = 3$). We just show the approximated Hamiltonian in CMS for $d = 2$ as follows,

$$\begin{pmatrix} m + \frac{p^2}{2m} & 0 & -i\frac{a_1 p_-}{\sqrt{2m}} & -i\frac{b_- p_-}{\sqrt{2m}} & -\frac{a_1 p_-}{2m} & -\frac{b_- p_-}{2m} \\ 0 & -m - \frac{p^2}{2m} & -i\frac{b_+ p_+}{\sqrt{2m}} & -i\frac{a_2 p_+}{\sqrt{2m}} & -\frac{b_+ p_+}{2m} & -\frac{a_2 p_+}{2m} \\ i\frac{a_1 p_+}{\sqrt{2m}} & i\frac{b_- p_-}{\sqrt{2m}} & m & p_- & a_1 & b_- \\ i\frac{b_+ p_+}{\sqrt{2m}} & i\frac{a_2 p_-}{\sqrt{2m}} & p_+ & -m & b_+ & a_2 \\ -\frac{a_1 p_+}{2m} & -\frac{b_- p_-}{2m} & a_1 & b_- & m & p_- \\ -\frac{b_+ p_+}{2m} & -\frac{a_2 p_-}{2m} & b_+ & a_2 & p_+ & -m \end{pmatrix}. \quad (42)$$

VIII. APPROXIMATION: PERTURBATION THEORY FOR THE CONSTRAINED SYSTEM

In this section, we use the standard perturbation theory to solve the RS eigen problem approximately. In 2D RS systems, by requiring \bar{H} contains the approximated eigenvectors of RS equations with the approximated eigenvalues, we can get $3 \times 3 \bar{H}(\mathbf{p})$ by separation of the positive and negative energy states as shown later. No matter for 2D or 3D RS systems, we conclude that we would get three equations for stationary states as follows,

$$h_{33}\phi_{3/2} + h_{31}\phi_{1/2} = \epsilon\phi_{3/2}, \quad (43)$$

$$h_{13}\phi_{3/2} + h_{11}\phi_{1/2} = \epsilon\phi_{1/2}, \quad (44)$$

$$H_{1/2}\phi_{1/2} = \epsilon\phi_{1/2}. \quad (45)$$

With the representation transformation R , we can use $\phi_{3/2}$, $\phi_{1/2}$ and ψ_{d+1} to represent the vector spinor ψ_μ . In the rest frame, i.e. $\mathbf{p} = (0, 0, 0)$ or $(0, 0)$ for $d = 3$ or 2 , the eigen solutions can be easily got and are denoted as $\epsilon_\pm^{(0)} = \pm m$. The corresponding eigenvectors are $(u_{\pm,3/2}^{(0)}, u_{\pm,1/2}^{(0)}, u_{t,\pm}^{(0)})^T$ where $u_{\pm,1/2}^{(0)} = u_{\pm,t}^{(0)} = (0, 0)^T$ or $(0, 0, 0, 0)^T$. We note that $u_{+,3/2}^{(0)} = (1, 0)^T$ and $u_{-,3/2}^{(0)} = (0, 1)^T$ for 2D systems and $u_{+,3/2}^{(0)} = e_1, e_2, e_3, e_4, u_{-,3/2}^{(0)} = e_5, e_6, e_7, e_8$ for 3D systems, where e_i is the i th column of $I_{8 \times 8}$. In the spirit of perturbation theory, we write (43-45) to the first order of $\frac{\mathbf{p}}{m}$,

$$h_{33}^{(0)} u_{\pm,3/2}^{(1)} + h_{33}^{(1)} u_{\pm,3/2}^{(0)} = \epsilon_\pm^{(0)} u_{\pm,3/2}^{(1)} + \epsilon_\pm^{(1)} u_{\pm,3/2}^{(0)}, \quad (46)$$

$$h_{13}^{(1)} u_{\pm,3/2}^{(0)} + h_{11}^{(0)} u_{\pm,1/2}^{(1)} = \epsilon_\pm^{(0)} u_{\pm,1/2}^{(1)}, \quad (47)$$

$$H_{1/2}^{(0)} u_{\pm,1/2}^{(1)} = \epsilon_\pm^{(0)} u_{\pm,1/2}^{(1)}. \quad (48)$$

By multiplying $u_{\pm,3/2}^{(0)}$ to the left side of (46), we find that $\epsilon_\pm^{(1)} = 0$ and multiplying $u_{\mp,3/2}^{(0)}$ to the left of (46), we find that $u_{\pm,3/2}^{(1)} = \pm \frac{h_{33}^{(1)} u_{\pm,3/2}^{(0)}}{2m}$.

Similarly, according to (47) and (48), we find that, $u_{\pm,1/2}^{(1)} = \pm \frac{h_{13}^{(1)} u_{\pm,3/2}^{(0)}}{2m}$. To the second order, the eigenvalues are $\epsilon_\pm^{(2)} = \pm \frac{p^2}{2m}$.

Finally, for the 3D RS systems, to the second order, the eigenvalues become $m + \frac{p^2}{2m}$ and $-m - \frac{p^2}{2m}$. The corresponding eigenvectors, to the first order in $\frac{\mathbf{p}}{m}$, are listed in the following table where $e'_i (i = 1, 2, 3, 4)$ are the i th column matrix of $I_{4 \times 4}$:

$u_{+,3/2}$	$u_{-,3/2}$	$u_{+,1/2}$
$(1, 0, 0, 0, (\frac{\Sigma^{\frac{3}{2}} \cdot \mathbf{p}}{2m} e'_1)^T)^T$	$(-(\frac{\Sigma^{\frac{3}{2}} \cdot \mathbf{p}}{2m} e'_1)^T, 1, 0, 0, 0)^T$	$(0, 0, (\frac{h'_{13}}{2m} e'_1)^T)^T$
$(0, 1, 0, 0, (\frac{\Sigma^{\frac{3}{2}} \cdot \mathbf{p}}{2m} e'_2)^T)^T$	$(-(\frac{\Sigma^{\frac{3}{2}} \cdot \mathbf{p}}{2m} e'_2)^T, 0, 1, 0, 0)^T$	$(0, 0, (\frac{h'_{13}}{2m} e'_2)^T)^T$
$(0, 0, 1, 0, (\frac{\Sigma^{\frac{3}{2}} \cdot \mathbf{p}}{2m} e'_3)^T)^T$	$(-(\frac{\Sigma^{\frac{3}{2}} \cdot \mathbf{p}}{2m} e'_3)^T, 0, 0, 1, 0)^T$	$(0, 0, (\frac{h'_{13}}{2m} e'_3)^T)^T$
$(0, 0, 0, 1, (\frac{\Sigma^{\frac{3}{2}} \cdot \mathbf{p}}{2m} e'_4)^T)^T$	$(-(\frac{\Sigma^{\frac{3}{2}} \cdot \mathbf{p}}{2m} e'_4)^T, 0, 0, 0, 1)^T$	$(0, 0, (\frac{h'_{13}}{2m} e'_4)^T)^T$
$u_{-,1/2}$	$u_{+,t}$	$u_{-,t}$
$(-\frac{h'_{13}}{2m} e'_1)^T, 0, 0)^T$	$(-i\sqrt{3}(\frac{h'_{13}}{2m} e'_1)^T, 0, 0)^T$	$(0, 0, i(\sqrt{3}\frac{h'_{13}}{2m} e'_1)^T)^T$
$(-\frac{h'_{13}}{2m} e'_2)^T, 0, 0)^T$	$(-i\sqrt{3}(\frac{h'_{13}}{2m} e'_2)^T, 0, 0)^T$	$(0, 0, i\sqrt{3}(\frac{h'_{13}}{2m} e'_2)^T)^T$
$(-\frac{h'_{13}}{2m} e'_3)^T, 0, 0)^T$	$(-i\sqrt{3}(\frac{h'_{13}}{2m} e'_3)^T, 0, 0)^T$	$(0, 0, i\sqrt{3}(\frac{h'_{13}}{2m} e'_3)^T)^T$
$(-\frac{h'_{13}}{2m} e'_4)^T, 0, 0)^T$	$(-i\sqrt{3}(\frac{h'_{13}}{2m} e'_4)^T, 0, 0)^T$	$(0, 0, i\sqrt{3}(\frac{h'_{13}}{2m} e'_4)^T)^T$

For the 2D RS systems, to the second order of $\frac{\mathbf{p}}{m}$, the eigenvalues become $m + \frac{p^2}{m}$ and $-m - \frac{p^2}{m}$ while to the first order of $\frac{\mathbf{p}}{m}$, the eigenvectors become, $u_{+,3/2} \approx (1, 0)$, $u_{-,3/2} \approx (0, 1)$, $u_{+,1/2} \approx (\frac{p_+}{2m}, 0)$, $u_{-,1/2} \approx (0, \frac{p_-}{2m})$, $u_{+,t} \approx -i\sqrt{2}(\frac{p_+}{2m}, 0)$ and $u_{-,t} \approx -i\sqrt{2}(0, \frac{p_-}{2m})$, respectively. We find that under such approximations, for a finite \mathbf{p} , the positive and negative energy sectors in the 2D RS systems are separated while in the 3D RS systems, they are not.

Let $H'_{3/2} = H'_{1/2} = H'_t = \text{diag}(m + \frac{p^2}{2m}, -m - \frac{p^2}{2m})$, and $R'_{13} = \text{diag}(\frac{p_+}{2m}, \frac{p_-}{2m})$, $R'_{t1} = -i\sqrt{2}$. We can find that the eigenvectors of $H'_{3/2}$ is just $(1, 0)^T$ or $(0, 1)^T$ with eigenvalues $m + \frac{p^2}{2m}$ or $-m - \frac{p^2}{2m}$, respectively. Then $R'_{13}(1, 0)^T(R'_{t1}R'_{13}(1, 0)^T)$ and $R'_{13}(0, 1)^T(R'_{t1}R'_{13}(0, 1)^T)$ are the eigenvectors of $H'_1(H'_t)$ with eigenvalues $m + \frac{p^2}{2m}$ or $-m - \frac{p^2}{2m}$, respectively. According to this fact, we then can construct a Hamiltonian in CMS which contains the ap-

proximative solutions in the 2D RS systems while it is difficult for three dimensions. We find that $\bar{H}'_{1t} = \begin{pmatrix} a_1 & b_- \\ b_+ & a_2 \end{pmatrix}$ where $b_{\pm} = b_1 \pm ib_2$ and a_1, a_2, b_1, b_2 are all real parameters. We take them real constants for simplicity. With this choice, we have $\bar{H}'_{31} = -i\sqrt{2} \begin{pmatrix} a_1 \frac{p_-}{2m} & b_- \frac{p_-}{2m} \\ b_+ \frac{p_+}{2m} & a_2 \frac{p_+}{2m} \end{pmatrix}$, and $\bar{H}'_{3t} = \begin{pmatrix} -a_1 \frac{p_-}{2m} & -b_- \frac{p_-}{2m} \\ -b_+ \frac{p_+}{2m} & -a_2 \frac{p_+}{2m} \end{pmatrix}$. Finally, The constructed $\mathbf{k} \cdot \mathbf{p}$ Hamiltonian in CMS is given by

$$\begin{pmatrix} m + \frac{p^2}{2m} & 0 & -i\frac{a_1 p_-}{\sqrt{2m}} & -i\frac{b_- p_-}{\sqrt{2m}} & -\frac{a_1 p_-}{2m} & -\frac{b_- p_-}{2m} \\ 0 & -m - \frac{p^2}{2m} & -i\frac{b_+ p_+}{\sqrt{2m}} & -i\frac{a_2 p_+}{\sqrt{2m}} & -\frac{b_+ p_+}{2m} & -\frac{a_2 p_+}{2m} \\ i\frac{a_1 p_+}{\sqrt{2m}} & i\frac{b_- p_-}{\sqrt{2m}} & m + \frac{p^2}{2m} & 0 & a_1 & b_- \\ i\frac{b_+ p_+}{\sqrt{2m}} & i\frac{a_2 p_-}{\sqrt{2m}} & 0 & -m - \frac{p^2}{2m} & b_+ & a_2 \\ -\frac{a_1 p_+}{2m} & -\frac{b_- p_-}{2m} & a_1 & b_- & m + \frac{p^2}{2m} & 0 \\ -\frac{b_+ p_+}{2m} & -\frac{a_2 p_-}{2m} & b_+ & a_2 & 0 & -m - \frac{p^2}{2m} \end{pmatrix} \quad (49)$$

When $b_1 = b_2 = 0$, we find that the positive and negative sectors are separated. By changing the order of the basis set,

the above Hamiltonian is in a block form, $\begin{pmatrix} H_+ & 0 \\ 0 & H_- \end{pmatrix}$, where, $H_+ = (m + \frac{p^2}{2m})I_{3 \times 3} + a_1 \begin{pmatrix} 0 & -i\frac{p_-}{\sqrt{2m}} & -\frac{p_-}{2m} \\ i\frac{p_+}{\sqrt{2m}} & 0 & 1 \\ -\frac{p_+}{2m} & 1 & 0 \end{pmatrix}$

and $H_- = (-m - \frac{p^2}{2m})I_{3 \times 3} + a_2 \begin{pmatrix} 0 & -i\frac{p_+}{\sqrt{2m}} & -\frac{p_+}{2m} \\ i\frac{p_-}{\sqrt{2m}} & 0 & 1 \\ -\frac{p_-}{2m} & 1 & 0 \end{pmatrix}$. With respect to a unitary transformation U which doesn't depend on \mathbf{p} ,

$$H'_+ = U^\dagger H_+ U = (m + \frac{p^2}{2m})I_{3 \times 3} + a_1 \begin{pmatrix} 0 & -\sqrt{\frac{3}{8}}\frac{p_-}{m} & -\sqrt{\frac{3}{8}}\frac{p_-}{m} \\ -\sqrt{\frac{3}{8}}\frac{p_+}{m} & 1 & 0 \\ -\sqrt{\frac{3}{8}}\frac{p_+}{m} & 0 & -1 \end{pmatrix}, \quad (50)$$

and

$$H'_- = U^\dagger H_- U = \left(-m - \frac{p^2}{2m}\right) I_{3 \times 3} + a_2 \begin{pmatrix} 0 & -\sqrt{\frac{3}{8}} \frac{p_+}{m} & -\sqrt{\frac{3}{8}} \frac{p_+}{m} \\ -\sqrt{\frac{3}{8}} \frac{p_-}{m} & 1 & 0 \\ -\sqrt{\frac{3}{8}} \frac{p_-}{m} & 0 & -1 \end{pmatrix}, \quad (51)$$

with $U = \begin{pmatrix} 1 & 0 & 0 \\ 0 & \frac{e^{-i\theta}}{\sqrt{2}} & -\frac{e^{i\theta}}{\sqrt{2}} \\ 0 & \frac{e^{-i\theta}}{\sqrt{2}} & \frac{e^{i\theta}}{\sqrt{2}} \end{pmatrix}$ and $\arctan \theta = \sqrt{2}$.

Notice that we have used the units $c = \hbar = 1$. After restoring the units, we have

$$H'_\pm = \left(\pm \frac{\hbar^2 q^2}{2m}\right) I_{3 \times 3} + a_\pm \begin{pmatrix} 0 & -\sqrt{\frac{3}{8}} \frac{\hbar q_\mp}{mc} & -\sqrt{\frac{3}{8}} \frac{\hbar q_\mp}{mc} \\ -\sqrt{\frac{3}{8}} \frac{\hbar q_\pm}{mc} & 1 & 0 \\ -\sqrt{\frac{3}{8}} \frac{\hbar q_\pm}{mc} & 0 & -1 \end{pmatrix}, \quad (52)$$

where we have neglected the energy constant $\pm m$, $a_+ = a_1, a_- = a_2$ and $\mathbf{p} = \hbar \mathbf{q}$. Denoting $\Delta_1 = \pm \frac{\hbar^2}{2m}, \Delta_2 = -a_\pm \sqrt{\frac{3}{8}} \frac{\hbar}{mc}, \Delta_3 = a_\pm$, the above Hamiltonians are rewritten as

$$H'_\pm = \begin{pmatrix} \Delta_1(q_x^2 + q_y^2) & \Delta_2 q_\mp & \Delta_2 q_\mp \\ \Delta_2 q_\pm & \Delta_1(q_x^2 + q_y^2) + \Delta_3 & 0 \\ \Delta_2 q_\pm & 0 & \Delta_1(q_x^2 + q_y^2) - \Delta_3 \end{pmatrix}. \quad (53)$$

Interestingly, in terms of Δ_i , we can get the effective mass and light velocity that, $m = |\frac{\hbar^2}{2\Delta_1}|$ and $c = |\sqrt{\frac{3}{2}} \frac{\Delta_1 \Delta_3}{\Delta_2 \hbar}|$.

IX. BERRY CURVATURE AND VANISHING ORBITAL MAGNETIC MOMENT

In this section, we first give the details of calculating the Berry curvature and orbital magnetic moment of the RS band in $H'_+(\mathbf{q})$ of Eq. (53) (note that the procedure for $H'_-(q)$ is similar).

Diagonalizing H'_+ , we obtain its eigenvalues and eigenvectors as follows (assume $\Delta_3 > 0$. Once $\Delta_3 < 0$, we can exchange the second and third basis vectors to make $\Delta_3 > 0$): The eigenvalues are $\epsilon_{RS} = \Delta_1 q^2$ (RS band) and $\epsilon_\pm = \Delta_1 q^2 \pm \sqrt{\Delta_3^2 + 2\Delta_2^2 q^2}$ (non-RS bands), while the corresponding eigenvectors are then, $u_{RS} = N_{RS}(1, -\frac{\Delta_2}{\Delta_3} q_+, \frac{\Delta_2}{\Delta_3} q_+)^T$, $u_+ = N_+(\frac{2\Delta_2 q_-}{\Delta_3 + \lambda(q)}, 1, \frac{\lambda(q) - \Delta_3}{\lambda(q) + \Delta_3})^T$ and $u_- = N_-(\frac{2\Delta_2 q_-}{\Delta_3 + \lambda(q)}, -\frac{\lambda(q) - \Delta_3}{\lambda(q) + \Delta_3}, -1)^T$ where $\lambda(q) = \sqrt{\Delta_3^2 + 2\Delta_2^2 q^2}$ and N_{RS}, N_\pm are the normalization factors, $N_{RS} = \frac{1}{\sqrt{1 + 2\frac{\Delta_2^2 q^2}{\Delta_3^2}}}, N_\pm = \frac{\lambda + \Delta_3}{2\lambda}$.

Then we can make a direct calculation according to $\Omega_n^z = i(\langle \partial_{q_x} u_n | \partial_{q_y} u_n \rangle - c.c.)$ and $m_n^z = -\frac{i\epsilon}{2}(\langle \partial_{q_x} u_n | H - \epsilon_n | \partial_{q_y} u_n \rangle - c.c.)$ [3] where Ω_n^z and m_n^z are the Berry curvature and orbital magnetic moment for the n th band respectively while $H(\mathbf{q})$ and $\epsilon_n(\mathbf{q})$ are the Bloch Hamiltonian and the eigen-energies for the n th band, respectively. We then find that

$$\Omega_{RS}^z = -\frac{4\Delta_2^2 \Delta_3^2}{(\Delta_3^2 + 2\Delta_2^2 q^2)^2} = -2\Omega_+^z = -2\Omega_-^z,$$

$$m_{RS}^z = 0, m_+^z = \frac{e\Delta_2^2 \Delta_3^2}{(\Delta_3^2 + 2\Delta_2^2 q^2)^{3/2}} = -m_-^z,$$

where the orbital magnetic moment for the RS band is always vanishing while its Berry curvature is not. This is totally different from the case for the massive Dirac quasiparticles where the orbital magnetic moment is proportional

to the Berry curvature [3]. Actually the peculiarity is originated from the non-trivial constraints in the RS equations. Another form of the formulas for Ω_n^z and m_n^z will help us to understand this peculiarity:

$$\Omega_n^z = i \sum_{n'} \left[\frac{\langle u_n | \partial_{q_x} H | u_{n'} \rangle \langle u_{n'} | \partial_{q_y} H | u_n \rangle}{(\epsilon_n - \epsilon_{n'})^2} - c.c. \right], \quad (54)$$

$$m_n^z = \frac{ie}{2} \sum_{n'} \left(\frac{\langle u_n | \partial_{q_x} H | u_{n'} \rangle \langle u_{n'} | \partial_{q_y} H | u_n \rangle}{\epsilon_n - \epsilon_{n'}} - c.c. \right). \quad (55)$$

As $\partial_{q_x} H'_+ = 2\Delta_1 q_x I_{3 \times 3} + \Delta_2 \begin{pmatrix} 0 & 1 & 1 \\ 1 & 0 & 0 \\ 1 & 0 & 0 \end{pmatrix}$, $\partial_{q_y} H'_+ = 2\Delta_1 q_y I_{3 \times 3} + \Delta_2 \begin{pmatrix} 0 & -i & -i \\ i & 0 & 0 \\ i & 0 & 0 \end{pmatrix}$, we will get,

$$\langle u_{RS} | \partial_{q_x} H'_+ | u_+ \rangle = \frac{\Delta_2}{\sqrt{1 + \frac{2\Delta_2^2 q^2}{\Delta_3^2}}}, \quad (56)$$

$$\langle u_{RS} | \partial_{q_y} H'_+ | u_+ \rangle = \frac{-i\Delta_2}{\sqrt{1 + \frac{2\Delta_2^2 q^2}{\Delta_3^2}}}, \quad (57)$$

$$\langle u_{RS} | \partial_{q_x} H'_+ | u_- \rangle = -\frac{\Delta_2}{\sqrt{1 + \frac{2\Delta_2^2 q^2}{\Delta_3^2}}}, \quad (58)$$

$$\langle u_{RS} | \partial_{q_y} H'_+ | u_- \rangle = \frac{i\delta_2}{\sqrt{1 + \frac{2\Delta_2^2 q^2}{\Delta_3^2}}}. \quad (59)$$

Then it is easy to find that,

$$\langle u_{RS} | \partial_{q_x} H'_+ | u_+ \rangle \langle u_+ | \partial_{q_y} H'_+ | u_{RS} \rangle = \langle u_{RS} | \partial_{q_x} H'_+ | u_- \rangle \langle u_- | \partial_{q_y} H'_+ | u_{RS} \rangle = \frac{i\Delta_2^2}{1 + 2\frac{\Delta_2^2 q^2}{\Delta_3^2}}. \quad (60)$$

According to Eq. (54), we can write Ω_{RS}^z as the sum of the contributions from u_+ and u_- :

$$\Omega_{RS}^z = \Omega_{RS,+}^z + \Omega_{RS,-}^z,$$

where, $\Omega_{RS,+}^z = -2Im \left[\frac{\langle u_{RS} | \partial_{q_x} H'_+ | u_+ \rangle \langle u_+ | \partial_{q_y} H'_+ | u_{RS} \rangle}{(\epsilon_{RS} - \epsilon_+)^2} \right]$, and $\Omega_{RS,-}^z = -2Im \left[\frac{\langle u_{RS} | \partial_{q_x} H'_+ | u_- \rangle \langle u_- | \partial_{q_y} H'_+ | u_{RS} \rangle}{(\epsilon_{RS} - \epsilon_-)^2} \right]$. They are equal, because according to Eq. (60), the denominators of $\Omega_{RS,+}^z$ and $\Omega_{RS,-}^z$ are the same while the numerators, i.e., $(\epsilon_{RS} - \epsilon_{\pm})^2$, are also the same. The contributions from u_{\pm} are additive, i.e., $\Omega_{RS,+}^z = \Omega_{RS,-}^z = -\frac{2\Delta_2^2 \Delta_3^2}{(\Delta_3^2 + 2\Delta_2^2 q^2)^2}$, then, $\Omega_{RS}^z = -\frac{4\Delta_2^2 \Delta_3^2}{(\Delta_3^2 + 2\Delta_2^2 q^2)^2}$.

However, the contributions from u_{\pm} to the orbital magnetic moment of the RS band are subtractive. According to Eq. (55),

$$m_{RS}^z = m_{RS,+}^z + m_{RS,-}^z,$$

where, $m_{RS,+}^z = -eIm \left(\frac{\langle u_{RS} | \partial_{q_x} H'_+ | u_+ \rangle \langle u_+ | \partial_{q_y} H'_+ | u_{RS} \rangle}{\epsilon_{RS} - \epsilon_+} \right)$, and $m_{RS,-}^z = -eIm \left(\frac{\langle u_{RS} | \partial_{q_x} H'_+ | u_- \rangle \langle u_- | \partial_{q_y} H'_+ | u_{RS} \rangle}{\epsilon_{RS} - \epsilon_-} \right)$. They are opposite in sign, because according to Eq. (60), the denominators of $m_{RS,+}^z$ and $m_{RS,-}^z$ are the same while the numerators, i.e., $\epsilon_{RS} - \epsilon_{\pm}$, are opposite in sign. Then $m_{RS,+}^z = -\frac{2e\Delta_2^2 \Delta_3^2}{(\Delta_3^2 + 2\Delta_2^2 q^2)^{3/2}} = -m_{RS,-}^z$, so $m_{RS}^z = 0$.

We now try to give the generic criterion for the vanishing orbital magnetic moment. One can always rewrite an arbitrary $s \times s$ Hamiltonian $H_{s \times s}(\mathbf{q})$ ($s = 2N + 1$, $N > 0$ is an integer) as $H_{s \times s}(\mathbf{q}) = h_{s \times s}(\mathbf{q}) + C(\mathbf{q})I_{s \times s}$ ($C(\mathbf{q})$ is just a scalar quantity). Assuming that we can find a constant unitary matrix $T_{s \times s}$ so that $h(\mathbf{q})$ satisfies

$$T^\dagger h(\mathbf{q})T = -h(\mathbf{q}), \quad (61)$$

and there is no degeneracy. Eq. (61) means that

$$T^\dagger(H(\mathbf{q}) - C(\mathbf{q}))T = -(H(\mathbf{q}) - C(\mathbf{q})), \quad (62)$$

i.e.,

$$T^\dagger H(\mathbf{q})T = 2C(\mathbf{q}) - H(\mathbf{q}). \quad (63)$$

Suppose $|u\rangle$ is the eigenvector of H , i.e., $H|u\rangle = \epsilon|u\rangle$, then $T|u\rangle$ would also be an eigenvector, $HT|u\rangle = (2C - \epsilon)T|u\rangle$ according to Eq. (63). Then the eigenvectors will be coming in pairs while the one with eigenvalue C has no partner. Hence, the eigenvectors can be labeled by N_3 : $H|u_{N_3}\rangle = \epsilon_{N_3}|u_{N_3}\rangle$ where $N_3 = -N, -N+1, \dots, N-1, N$ with $\epsilon_{-N_3} = 2C - \epsilon_{N_3}$ and T connects a state $|u\rangle$ with its partner, namely,

$$T|u_{N_3}\rangle = |u_{-N_3}\rangle. \quad (64)$$

Consequently,

$$T^\dagger(H - \epsilon_{N_3})T = -(H - \epsilon_{-N_3}). \quad (65)$$

Thus the orbital magnetic moments are restricted to satisfy $m_{-N_3}^z = -m_{N_3}^z$. The reason is that,

$$\begin{aligned} m_{-N_3}^z &= -\frac{ie}{2}(\langle \partial_{q_x} u_{-N_3} | H(\mathbf{q}) - \epsilon_{-N_3}(\mathbf{q}) | \partial_{q_y} u_{-N_3} \rangle - c.c.) = \\ &\frac{ie}{2}(\langle \partial_{q_x} u_{-N_3} | T^\dagger(H(\mathbf{q}) - \epsilon_{N_3}(\mathbf{q}))T | \partial_{q_y} u_{-N_3} \rangle - c.c.) = \\ &\frac{ie}{2}(\langle \partial_{q_x} u_{N_3} | H(\mathbf{q}) - \epsilon_{N_3}(\mathbf{q}) | \partial_{q_y} u_{N_3} \rangle - c.c.) = -m_{N_3}^z, \end{aligned}$$

where we have used the relation $T\partial_{\mathbf{q}}|u_{N_3}\rangle = \partial_{\mathbf{q}}|u_{-N_3}\rangle$ according to Eq. (64).

Thus $m_0^z = 0$, i.e., the orbital magnetic moment of the middle band is restricted to be vanishing. On the other hand, it is similar to find that $\Omega_{-N_3}^z = \Omega_{N_3}^z$, which won't restrict Ω_0^z to be zero.

We can also write m_0^z as the contributions from the other bands, i.e.,

$$m_0^z = (m_{0,+1}^z + m_{0,-1}^z) + (m_{0,+2}^z + m_{0,-2}^z) + \dots + (m_{0,+N}^z + m_{0,-N}^z).$$

For each parenthesis $(m_{0,N'}^z, m_{0,-N'}^z)$ where $N' = 1, 2, \dots, N$, $m_{0,N'}^z = -m_{0,-N'}^z$, then they are subtractive and $m_0^z = 0$. This is because,

$$\begin{aligned} m_{0,N'}^z &= -eIm\left(\frac{\langle u_0 | \partial_{q_x} H | u_{N'} \rangle \langle u_{N'} | \partial_{q_y} H | u_0 \rangle}{\epsilon_0 - \epsilon_{N'}}\right), \\ m_{0,-N'}^z &= -eIm\left(\frac{\langle u_0 | \partial_{q_x} H | u_{-N'} \rangle \langle u_{-N'} | \partial_{q_y} H | u_0 \rangle}{\epsilon_0 - \epsilon_{-N'}}\right). \end{aligned}$$

As $\epsilon_0 = C, \epsilon_{N'} = 2C - \epsilon_{-N'}$, the numerators, i.e., $\epsilon_0 - \epsilon_{-N'} = -(\epsilon_0 - \epsilon_{N'})$. As $u_{-N'} = Tu_{N'}, u_0 = Tu_0$, then, the denominators,

$$\langle u_0 | \partial_{q_x} H | u_{-N'} \rangle \langle u_{-N'} | \partial_{q_y} H | u_0 \rangle = \langle u_0 | T^\dagger \partial_{q_x} HT | u_{N'} \rangle \langle u_{N'} | T^\dagger \partial_{q_y} HT | u_0 \rangle.$$

According to Eq. (63), $T^\dagger \partial_{q_x} HT = 2\partial_{q_x} C - \partial_{q_x} H, T^\dagger \partial_{q_y} HT = 2\partial_{q_y} C - \partial_{q_y} H$, then,

$$\langle u_0 | \partial_{q_x} H | u_{-N'} \rangle \langle u_{-N'} | \partial_{q_y} H | u_0 \rangle = \langle u_0 | \partial_{q_x} H | u_{N'} \rangle \langle u_{N'} | \partial_{q_y} H | u_0 \rangle,$$

where we have used the relation that $\langle u_0 | u_{N'} \rangle = 0$. Finally, $m_{0,N'}^z = -m_{0,-N'}^z$.

For $H'_+ = \Delta_1 q^2 I_{3 \times 3} + h$ in Eq. (53), we can find a T matrix, $T = \begin{pmatrix} 1 & 0 & 0 \\ 0 & 0 & -1 \\ 0 & -1 & 0 \end{pmatrix}$ so that $T^\dagger h T = -h$, and $C(\mathbf{q}) = \Delta_1 q^2$. We can then label the eigenvalues and eigenvectors of H'_+ by $N_3 = 0, \pm$, i.e., $u_{RS} \equiv u_0$ while $\epsilon_{RS} \equiv \epsilon_0$. It is easy to find that $T u_\pm = u_\mp$ and $T u_{RS} = u_{RS}$. According to the above arguments, we can find that m_{RS}^z is restricted to be zero while Ω_{RS}^z is not, which is consistent with the direct calculation.

X. MATERIAL REALIZATIONS: SYMMETRY REQUIREMENTS

In order to get the 2D RS excitations in CMS, we firstly consider the generic Hamiltonian (Eq. (53)) in the following form:

$$\mathcal{H}(q_x, q_y) = \begin{pmatrix} \Delta_1(q_x^2 + q_y^2) + E_1 & \Delta_2 q_\mp & \Delta_2 q_\mp \\ \Delta_2 q_\pm & \Delta_1(q_x^2 + q_y^2) + E_2 & \Delta_{23} \\ \Delta_2 q_\pm & \Delta_{23} & \Delta_1(q_x^2 + q_y^2) + E_3 \end{pmatrix}, \quad (66)$$

where $q_\pm = q_x \pm i q_y$ and $\Delta_1, \Delta_2, \Delta_{23}, E_1, E_2, E_3$ are all real parameters with appropriate units. As we know, symmetries of Hamiltonian always add some restrictions to the form of the low energy $\mathbf{k} \cdot \mathbf{p}$ Hamiltonian around the point of symmetry \mathbf{k}^* in the Brillouin zone (BZ), because the Bloch Hamiltonian $H(\mathbf{k})$ satisfies [4],

$$D(\{\alpha|\mathbf{t}\})^\dagger H(\alpha\mathbf{k}) D(\{\alpha|\mathbf{t}\}) = H(\mathbf{k}), \quad (67)$$

where $\{\alpha|\mathbf{t}\}$ is an element of the space group, and $D(\{\alpha|\mathbf{t}\})$ is a matrix representation. It is obvious that any operation in the translation group, namely $\{E|\mathbf{R}_l\}$ in T , will not produce any restriction according to Eq. (67). For \mathbf{k}^* , any other symmetry operations $\{\beta|\mathbf{t}'\}$ will produce symmetry restrictions to $H(\mathbf{k}^*)$ when $\beta\mathbf{k}^* = \mathbf{k}^* + \mathbf{G}$ where \mathbf{G} is a reciprocal lattice vector. The rest symmetry operations in the space group will generate a wave vector star, and relate the low energy models around these vectors in the star with each other. Writing $\mathbf{q} = \mathbf{k} - \mathbf{k}^*$, and for $\{\beta|\mathbf{t}'\}$, we can find that,

$$D(\{\beta|\mathbf{t}'\})^\dagger H(\mathbf{k}^* + \mathbf{G} + \beta\mathbf{q}) D(\{\beta|\mathbf{t}'\}) = H(\mathbf{k}^* + \mathbf{q}). \quad (68)$$

As $H(\mathbf{k} + \mathbf{G})$ is related to $H(\mathbf{k})$ by a unitary transformation which can be absorbed in D , we can get the following equation,

$$\mathcal{D}(\{\beta|\mathbf{t}'\})^\dagger \mathcal{H}(\beta\mathbf{q}) \mathcal{D}(\{\beta|\mathbf{t}'\}) = \mathcal{H}(\mathbf{q}), \quad (69)$$

where $\mathcal{H}(\mathbf{q}) \equiv H(\mathbf{k}^* + \mathbf{q})$ and \mathcal{D} is the representation of the symmetry group of \mathbf{k}^* , which can be derived based on group theory.

Based on the above equation, we will reveal the symmetry requirements for getting the low energy Hamiltonian $\mathcal{H}(\mathbf{q})$ as shown in Eq. (66) step by step. Inspired by the 2D RS equations which describes that three Dirac spinors obey Dirac equation with nontrivial constraints, for the material realizations, we can consider three 2D layers each of which will provide a q^2 -like excitation firstly, and then consider the coupling between these layers. We consider nonmagnetic materials with negligible spin orbit coupling for simplicity.

Around z -axis, \mathbf{k}^* of a layer can be subject to C_n point symmetry cyclic group [5], whose irreducible representation (IR) can be denoted by l_z where $l_z = 1, 2, \dots, n$ and the corresponding transformation matrix is just a number: $\mathcal{D}(c_n) = e^{-i\frac{2\pi l_z}{n}}$ where c_n denotes the rotation around z -axis by an angle $\frac{2\pi}{n}$. Using Eq. (69), we can find that $n = 3, 4, 6$, because C_1 would allow the first order of \mathbf{q} while C_2 would allow the different coefficients before q_x^2 and q_y^2 . We choose the basis sets located at the three layer respectively, i.e., the one in the middle or second layer corresponds to the first basis vector while the one in the first (third) layer corresponds to the second (third) basis

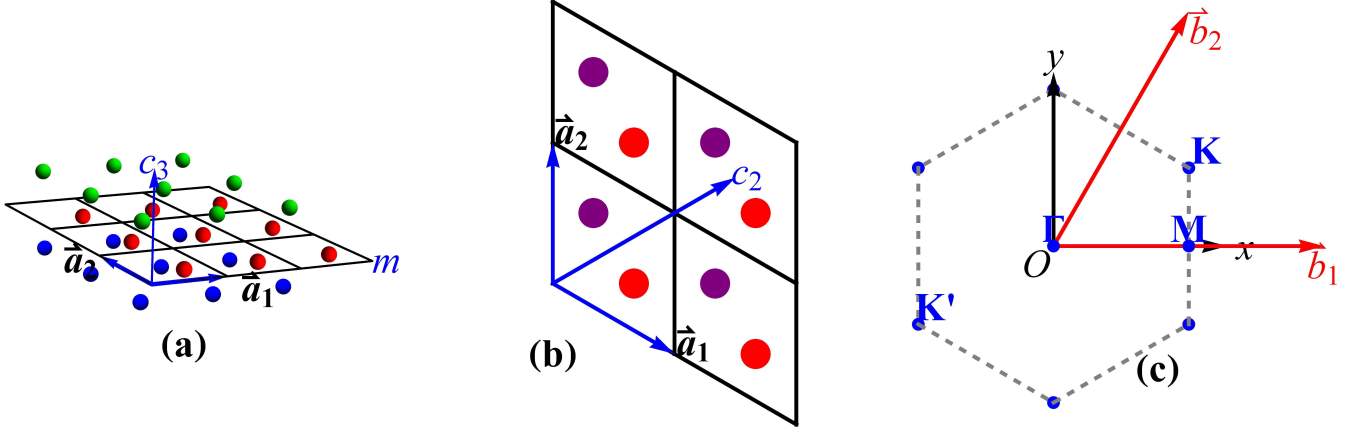


Fig. S 1: In (a), we show the prototypical structure with a triangular lattice. \mathbf{a}_1 and \mathbf{a}_2 are primitive lattice basis vectors, and c_3 is along the z -axis which is perpendicular to the both \mathbf{a}_1 and \mathbf{a}_2 . The first layer is depicted in green, the second layer is depicted in red, while the third layer is depicted in blue, and each ball represents an atom. (b) shows the top view, where the red disks shows the atoms in the second layer while the purple ones are the atoms in the first or the third layers. The second layer is a mirror plane which relate the first and third layer. In (c), we show the hexagonal BZ where \mathbf{b}_1 and \mathbf{b}_2 are reciprocal basis vectors. In (b), we also show a rotation c_2 which is not the symmetry operation of the lattice in (a), but can relate the first and second layer when located at the middle plane between the first and second layer.

vector. The relatively large distance between the first and third layers guarantees that the coupling between the corresponding basis vectors is small, i.e., Δ_{23} can be negligible which is required by the RS physics.

Next we consider the simulation of \mathcal{H}_{12} and \mathcal{H}_{13} . According to Eq. (69), we can find that, for the coupling $\mathcal{H}_{12} = \mathcal{H}_{13} \sim q_{\mp}$, the IR in the second layer l_z^2 and in the first (third) layer l_z^1 (l_z^3) should satisfy $l_z^2 - l_z^1 = l_z^2 - l_z^3 = \pm 1$. The realization of such a relation between the IR's in different layers is subtle because it is through the displacement in the xy -plane between the different layers, which guarantees that the IR's are different. We denote such a displacement from the second layer to the first (third) layer as δ (δ'), it is easy to show that for c_n (with respect to the second layer, i.e., the fixed point is at some atom in the second layer) to survive, $c_n \delta - \delta = \mathbf{R}_l$, $c_n \delta' - \delta' = \mathbf{R}'_l$ where $\mathbf{R}_l, \mathbf{R}'_l$ are lattice vectors. Suppose the Bloch function $\psi_{\mathbf{k}^*}(\mathbf{r})$ (which satisfies $\psi_{\mathbf{k}^*}(\mathbf{r} - \mathbf{R}_l) = e^{-i\mathbf{k}^* \cdot \mathbf{R}_l} \psi_{\mathbf{k}^*}(\mathbf{r})$) is the basis vector in the second layer with the property that $c_n \psi_{\mathbf{k}^*}(\mathbf{r}) = \psi_{\mathbf{k}^*}(c_n^{-1} \mathbf{r}) = \chi \psi_{\mathbf{k}^*}(\mathbf{r})$. Then in the first (third) layer, we will have $\psi_{\mathbf{k}^*}(\mathbf{r} - \delta)$ ($\psi_{\mathbf{k}^*}(\mathbf{r} - \delta')$), which satisfies that,

$$c_n \psi_{\mathbf{k}^*}(\mathbf{r} - \delta(\delta')) = \psi_{\mathbf{k}^*}(c_n^{-1} \mathbf{r} - \delta(\delta')) = e^{i\mathbf{G} \cdot \delta(\delta')} \chi \psi_{\mathbf{k}^*}(\mathbf{r} - \delta(\delta')), \quad (70)$$

where $c_n \mathbf{k}^* = \mathbf{k}^* + \mathbf{G}$. Therefore, we will have,

$$\mathbf{G} \cdot \delta = \mathbf{G} \cdot \delta' = \pm \frac{2\pi}{n}, \quad (71)$$

which rules out the Γ point and require that \mathbf{k}^* should be located at the boundary of the BZ. Furthermore, the point group of \mathbf{k}^* should be only C_3 , because C_6 will require that \mathbf{k}^* is Γ and C_4 is also ruled out for only $(\frac{1}{2}, \frac{1}{2})$ in the BZ of square lattice owns C_4 symmetry and is located at the boundary of the BZ (giving a non-vanishing \mathbf{G}), however the displacement satisfying Eq. (71) will not let C_4 symmetry survive. For C_3 , \mathbf{k}^* can be K or K' and because K' is related to K by time-reversal symmetry, hereafter we just consider K shown in Fig. S 1(c), which is equal to $\frac{1}{3}\mathbf{b}_1 + \frac{1}{3}\mathbf{b}_2$. Obviously, $c_3 K = K - \mathbf{b}_1$, thus $\delta = \mp \frac{1}{3}\mathbf{a}_1 \pm \frac{1}{2}\mathbf{a}_2$. At last we require that the first layer should be related to the third layer by the mirror plane coincided with the second layer, which can guarantee that the coefficients before q_{\mp} in \mathcal{H}_{12} and \mathcal{H}_{13} are the same.

As a matter of fact, we can focus on the lattice model shown in Fig. S 1(a), whose primitive lattice basis vectors are denoted by \mathbf{a}_1 and \mathbf{a}_2 , and in the Cartesian coordinate system shown in Fig. S 1(c), $\mathbf{a}_1 = a(\frac{\sqrt{3}}{2}, -\frac{1}{2})$ and $\mathbf{a}_2 = a(0, 1)$ where a is the lattice parameter. Then we can get the reciprocal lattice basis vectors, $\mathbf{b}_1 = \frac{4\pi}{\sqrt{3}a}(1, 0)$ and $\mathbf{b}_2 = \frac{4\pi}{\sqrt{3}a}(\frac{1}{2}, \frac{\sqrt{3}}{2})$. The hexagonal BZ is shown in Fig. S 1(c), and we have labeled three points of symmetry,

Space group	Combination of Wyckoff positions	Space group	Combination of Wyckoff positions
P312	(1a, 2h), (1a, 2i), (1b, 2h), (1b, 2i) (1c, 2g), (1c, 2i), (1d, 2g), (1d, 2i) (1e, 2g), (1e, 2h), (1f, 2g), (1f, 2h)	P6 ₃ 22	(2b, 4f), (2c, 4e), (2d, 4e), (2d, 4f)
P-31c	(2a, 4f), (2c, 4e), (2d, 4e), (2d, 4f)	P-6m2	(1a, 2h), (1a, 2i), (1b, 2h), (1b, 2i) (1c, 2g), (1c, 2i), (1d, 2g), (1d, 2i) (1e, 2g), (1e, 2h), (1f, 2g), (1f, 2h)
P-6	(1a, 2h), (1a, 2i), (1b, 2h), (1b, 2i) (1c, 2g), (1c, 2i), (1d, 2g), (1d, 2i) (1e, 2g), (1e, 2h), (1f, 2g), (1f, 2h)	P-6c2	(2b, 4h), (2b, 4i), (2a, 4h), (2a, 4i) (2c, 4g), (2c, 4i), (2d, 4g), (2d, 4i) (2e, 4g), (2e, 4h), (2f, 4g), (2f, 4h)
P6 ₃ /m	(2a, 4f), (2c, 4e), (2d, 4e), (2d, 4f)	P-62c	(2b, 4f), (2c, 4e), (2d, 4e), (2d, 4f)
P6 ₃ /mmc	(2b, 4f), (2c, 4e), (2d, 4e), (2d, 4f)		

Table S I: The combination of different Wyckoff positions which will result in three iso-structure layers in one unit cell.

$\Gamma = (0, 0)$, $M = \frac{1}{2}\mathbf{b}_1$ and $K = -K' = \frac{1}{3}(\mathbf{b}_1 + \mathbf{b}_2)$. The three-layer structure shown in Fig. S 1(a) satisfies the requirements claimed before: each layer is a triangular lattice and each unit cell only contains one atom. According to such a prototypical structure, we then search the 3D space groups from No. 143 to No. 194 and get the combinations of Wyckoff positions which can give such a three-layer structure (or two) in a unit cell, as listed in Table S I. The combination like $(1a, 2h)$ means there is only one three-layer structure with the layer from $1a$ atoms being the middle layer while the combination like $(2b, 4f)$ mean there are two three-layer structures with $(2b)$ atoms forms two middle layers.

XI. COMPUTATIONAL METHOD

The electronic band structure calculations have been carried out using the full potential linearized augmented plane wave method as implemented in WIEN2K package [6]. We used the Perdew-Burke-Ernzerhof (PBE) generalized gradient approximation (GGA) exchange-correlation density functional [7]. A $12 \times 12 \times 1$ mesh is used for the Brillouin zone integral. A vacuum spacing of 20\AA is used so that the interaction in the non-periodic directions can be neglected.

-
- [1] See, e.g., D. Lurie, *Particles and Fields*, (John and Wiley Sons, New York, 1968).
[2] See, e.g., M. Maggiore, *A Modern Introduction to Quantum Field Theory*, (Oxford University Press, New York, 2005).
[3] D. Xiao, M.-C. Chang and Q. Niu, Berry phase effects on electronic properties, *Rev. Mod. Phys.* **82**, 1959-2007 (2010).
[4] See, e.g., Lok C. Lew Yan Voon and Morten Willatzen, *The $\mathbf{k}\cdot\mathbf{p}$ Method, Electronic Properties of Semiconductors*, (Springer-Verlag Berlin Heidelberg, 2009).
[5] See, e.g., C. J. Bradley and A. P. Cracknell, *The Mathematical Theory of Symmetry in Solids, Representation Theory for Point Groups and Space Groups*, (Oxford University Press, New York, 1972).
[6] P. Blaha, K. Schwarz, G. Madsen, D. Kvasicka and J. Luitz, WIEN2k, An Augmented Plane Wave Plus Local Orbitals Program for Calculating Crystal Properties, (2001).
[7] J. P. Perdew, K. Burke and M. Ernzerhof, Generalized Gradient Approximation Made Simple, *Phys. Rev. Lett.* **77**, 3865-3868 (1996).